AD-A237 680

NAVAL POSTGRADUATE SCHOOL
Monterey , California

DTIC
ELECTE
JUL 01 1991
S
C
D

THESIS

COMPUTOR MODEL OF THE PERFORMANCE OF A
THERMOACOUSTIC GENERATOR

by

Paul D. Fisher

June 1990

Thesis Advisor: A. A. Atchey
Co-Advisor: T. J. Hofler

91 6 24   068   91-03261

Unclassified

SECURITY CLASSIFICATION OF THIS PAGE

REPORT DOCUMENTATION PAGE

1a REPORT SECURITY CLASSIFICATION UNCLASSIFIED	1b RESTRICTIVE MARKINGS
2a SECURITY CLASSIFICATION AUTHORITY	3 DISTRIBUTION AVAILABILITY OF REPORT Approved for public release;
2b DECLASSIFICATION DOWNGRADING SCHEDULE	distribution is unlimited.

4 PERFORMING ORGANIZATION REPORT NUMBER(S)	5 MONITORING ORGANIZATION REPORT NUMBER(S)

6a NAME OF PERFORMING ORGANIZATION Naval Postgraduate School	6b OFFICE SYMBOL (if applicable) N33	7a NAME OF MONITORING ORGANIZATION Naval Postgraduate School
6c ADDRESS (City, State, and ZIP Code) Monterey, Ca. 93943-5000		7b ADDRESS (City, State, and ZIP Code) Monterey, Ca. 93943-5000

8a NAME OF FUNDING/SPONSORING ORGANIZATION	8b OFFICE SYMBOL (If applicable)	9 PROCUREMENT INSTRUMENT IDENTIFICATION NUMBER
8c ADDRESS (City, State, and ZIP Code)		10 SOURCE OF FUNDING NUMBERS

PROGRAM ELEMENT NO	PROJECT NO	TASK NO	WORK UNIT ACCESSION NO

11 TITLE (Include Security Classification)

COMPUTER MODEL OF THE PERFORMANCE OF A THERMOACOUSTIC GENERATOR (UNCLASSIFIED)

12 PERSONAL AUTHOR(S)
Fisher, Paul D.

13a TYPE OF REPORT Master's Thesis	13b TIME COVERED FROM _____ TO _____	14 DATE OF REPORT (Year, Month, Day) June 1990	15 PAGE COUNT 63

16 SUPPLEMENTARY NOTATION The views expressed in this thesis are those of the author and do not reflect the official policy or position of the Department of Defense or the U.S. Government.

17	COSATI CODES		18 SUBJECT TERMS (Continue on reverse if necessary and identify by block number)
FIELD	GROUP	SUB-GROUP	Thermoacoustics

19 ABSTRACT (Continue on reverse if necessary and identify by block number)

A computer program is developed to predict the performance of a thermoacoustic generator. The defining relationships are based on equations derived using short stack and boundary layer approximations. The engine modeled is the five inch engine currently in operation at Los Alamos National Laboratory. The working fluid in the model is a helium-argon gas mix, chosen to provide flexibility in placing the transducer relative to the thermoacoustic stack assembly while maintaining resonance near the desired operating frequency of 120 Hz. The transducer model is based on a linear alternator design proposed for use with the L. A. N. L. engine in the future. The thermodynamic properties of the gas mix are determined using virial equations and binary gas mixture relationships. The defining relations are solved simultaneously and an iterative process is used to optimize the gas mix. The variables for which the program then solves are pressure amplitude, hot heat exchanger temperature, and angular frequency as functions of input heat flux, system geometry, and load characteristics. From these, the power output and total system efficiency are determined.

20 DISTRIBUTION/AVAILABILITY OF ABSTRACT ☒ UNCLASSIFIED/UNLIMITED ☐ SAME AS RPT ☐ DTIC USERS	21 ABSTRACT SECURITY CLASSIFICATION Unclassified
22a NAME OF RESPONSIBLE INDIVIDUAL A. A. Atchley	22b TELEPHONE (Include Area Code) (408)646-2848	22c OFFICE SYMBOL 61Ay

DD FORM 1473, 84 MAR
83 APR edition may be used until exhausted
All other editions are obsolete

SECURITY CLASSIFICATION OF THIS PAGE

☆ U.S. Government Printing Office 1986—606-24

Unclassified

i

Computer Model of the Performance of a

Thermoacoustic Generator

by

Paul D. Fisher
Lieutenant, United States Navy
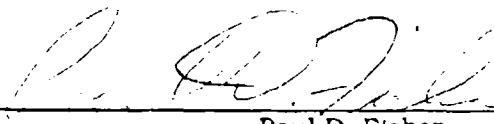B.S.E.S., Purdue University, 1981

Submitted in partial fulfillment of the
requirements for the degree of

MASTER OF SCIENCE IN PHYSICS

from the

NAVEL POSTGRADUATE SCHOOL
June 1990

Author: _____
Paul D. Fisher

Approved by: _____
A. A. Atchley, Thesis advisor

_____
T. J. Hofler, Second reader

_____
K. E. Woehler, Chairman
Department of Physics

Abstract

A computer program is developed to predict the performance of a thermoacoustic generator. The defining relationships are based on equations derived using short stack and boundary layer approximations. The engine modeled is the five inch engine currently in operation at Los Alamos National Laboratory. The working fluid in the model is a helium-argon gas mix, chosen to provide flexibility in placing the transducer relative to the thermoacoustic stack assembly while maintaining resonance near the desired operating frequency of 120 Hz. The transducer model is based on a linear alternator design proposed for use with the L. A. N. L. engine in the future. The thermodynamic properties of the gas mix are determined using virial equations and binary gas mixture relationships. The defining relations are solved simultaneously and an iterative process is used to optimize the gas mix. The variables for which the program then solves are pressure amplitude, hot heat exchanger temperature, and angular frequency as functions of input heat flux, system geometry, and load characteristics. From these, the power output and total system efficiency are determined.

TABLE OF CONTENTS

LIST OF SYMBOLS

Symbol	Definition
A, B	Complex pressure amplitudes
a, b	Real part of complex pressure amplitudes
c	Sound speed
C	Capacitance
c_p	Isobaric specific heat capacity
c_v	Isochoric specific heat capacity
d	Resonator diameter
f	Frequency or function
g	Geometry factor
H	Total energy flux
I	Electric current
Im	Imaginary part of
k	Wave number
K	Thermal conductivity
L	Plate half thickness or inductance
m	Mass
P, p	Pressure
q	Heat flux per unit area
Q	Heat flux
R	Resistance
Re	Real part of
s	Spring constant
S	Entropy flux
t	Time
T	Temperature
u	Velocity
V	Voltage
w	Power per unit volume
W	Work flux
x	Position
y_o	Plate half gap
Z	Impedance
α	Imaginary part of complex pressure amplitude A
β	Imaginary part of complex pressure amplitude B or thermal expansion coefficient
Γ	Normalized temperature gradient
γ	Specific heat capacity ratio
δ	Penetration depth
ε	Plate heat capacity ratio
η	Efficiency
κ	Thermal diffusivity
λ	Wavelength
μ	Dynamic viscosity

ν	Kinematic viscosity
ζ	Displacement
ξ	Second viscosity
Π	Power or perimeter
ρ	Density
σ	Prandtl number
ϕ	Phase angle
ω	Angular frequency

ACKNOWLEDGMENTS

The work presented in the following thesis was inspired in large part by Greg Swift. His assitance and guidance, especially in the early stages of the work. contributed enormously to the my understanding of the principles of thermoacoustics, and to my ability to apply them in a meaningful manner to solve the problems which were encountered in developing the computer model, which is the heart of this thesis. Conversations with Vince Kotsubo, William Ward, and William Wright were also extremely beneficial in defining the problem that I have attempted to solve. Finally, I wish to thank Anthony Atchley and Tom Hofler for their assistance and endless patience in the preparations of this work.

I. INTRODUCTION

A. OVERVIEW

A great deal of work has been done in the development of practical thermoacoustic refrigerators which use gas as a working fluid. Examples include the Thermoacoustic Refrigerator (Hofler, 1986) and the Space Thermoacoustic Refrigerator (Susalla, 1988). Work on thermoacoustic prime movers which use a gas as a working fluid consists primarily of enclosing the thermoacoustic engine in a tube with two rigid ends and measuring the performance of the engine under various pressure, temperature and geometry conditions. Relatively little work has been done in developing a thermoacoustic generator.

The history of thermoacoustics is long, but significant advances in practical thermoacoustic devices are relatively recent. As early as 1777, experiments were performed by Byron Higgins, in which acoustic oscillations were excited in a large pipe by suitable placement of an internal hydrogen flame (Putnam and Dennis, 1956). Higgens' work eventually led to the modern science of pulse combustion, whose applications have included the German V-1 rocket used in World War II and the residential pulse-combustion furnace introduced by Lennox, Inc. in 1982 (Swift, 1988).

The earliest antecedent of the thermoacoustic prime movers in use today is the Sondhauss tube. Over 100 years ago, it was observed that a hot glass bulb attached to a cool glass tube sometimes emitted sound at the tip of the tube. Sondhauss quantitatively investigated the relationship between the pitch of the sound emitted and the dimensions of the tube. Lord Rayleigh explained the Sondhauss tube qualitatively in 1896, but a quantitative theoretical description of these phenomena was not achieved until about 20 years ago when Rott and others published a series of papers (Swift, 1988). Rott's theory combines basic principles from physics,

thermodynamics, and acoustics to describe the effects found in both thermoacoustic prime movers and heat pumps.
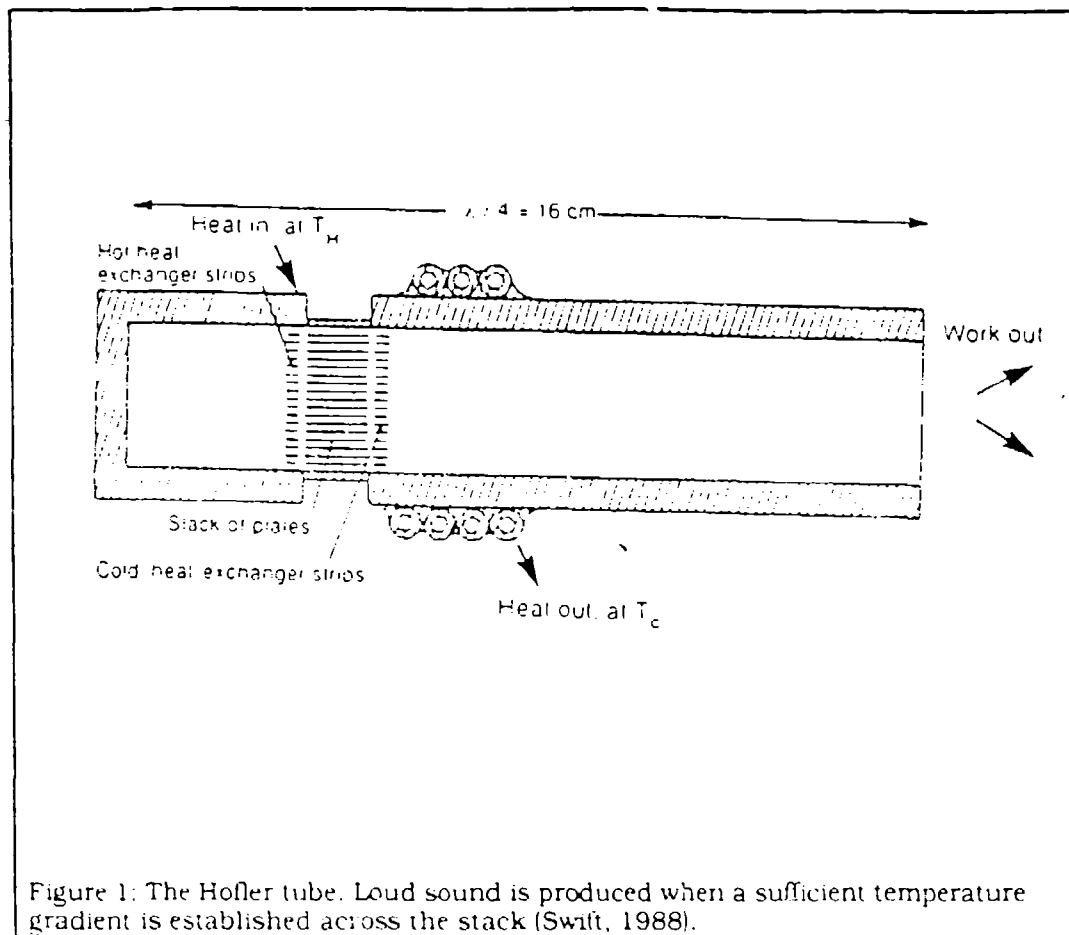
One of the most significant advances in experimental thermoacoustics was the realization, by Carter, White, and Steele of North American Aviation, Inc. in 1962, that placing structures (such as a stack of plates) inside a Sondhauss tube could improve the performance of the tube in generating sound (Swift, 1988).

In recent years, a number of people including Wheatley, Hofler, Swift, and Migliori, performed a series of experiments at Los Alamos National Laboratory (L.A.N.L.) in New Mexico. The purpose of the experiments was to investigate the thermoacoustic effects in both prime movers and heat pumps, and compare these experimental results to Rott's theory (Susalla, 1988).

The first acoustic heat pump built at L.A.N.L. consisted of a speaker mounted at one end of a closed tube which contained a stack of fiberglass plates positioned near the closed end. They found that a temperature difference of 100 degrees centigrade across the stack of plates was easily produced in about a minute with the speaker driving at acoustic resonance (Wheatly, Swift, and Migliori, 1986).

Shortly after the first heat pump was built at L.A.N.L., Hofler built a device, which has come to be known as the Hofler tube, to use as a demonstration for his Ph.D. candidacy committee at the University of California, San Diego. The device (Fig. 1) produces an impressive level of sound from the open end, about 100dB at one meter (Swift, 1988).

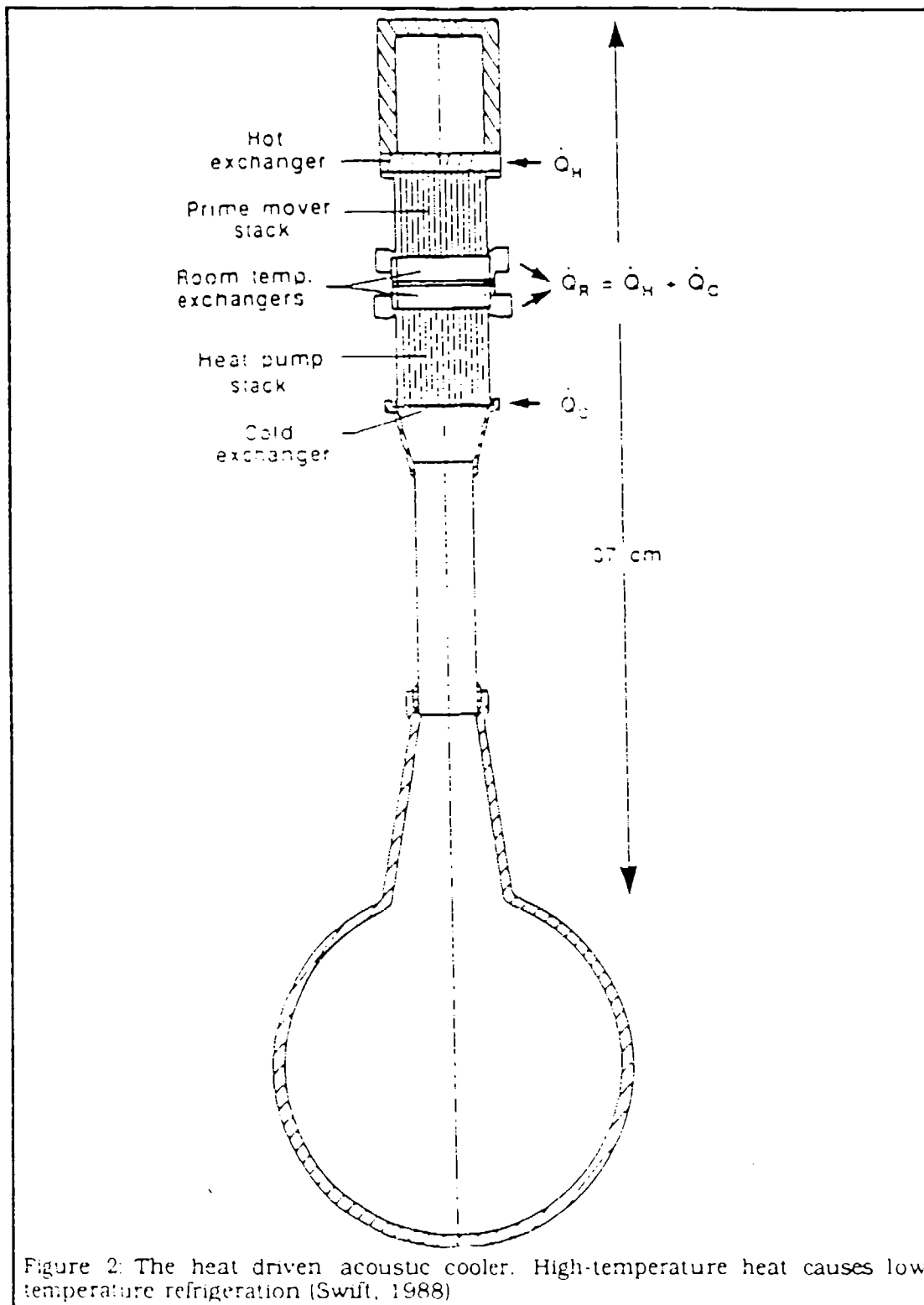Other devices built and studied at L.A.N.L. include Hofler's refrigerator, the heat-driven acoustic cooler (Fig. 2), a liquid sodium acoustic engine, and a liquid propylene engine (Wheatly, Swift, and Migliori, 1986). Currently being studied at L.A.N.L. is a five inch thermoacoustic prime mover, which will be described in detail later. It is the prime mover upon which the calculations described herin are based.

Figure 1: The Hofler tube. Loud sound is produced when a sufficient temperature gradient is established across the stack (Swift, 1988).

B. MOTIVATION

The results of these early experiments on thermoacoustic refrigerators at L.A.N.L. indicated a system performance that was far less than expected (Hofler, 1986). These results led Hofler to apply Rott's theory to the experimental systems, solving the resulting equations numerically. He also built the thermoacoustic refrigerator, made accurate measurements of it s thermodynamic efficiency, and compared these results to those predicted by theory. The work which followed at the Naval Postgraduate School by Susalla and others was done to improve the overall efficiency of the system and make it suitable for space applications (Susalla, 1986.

Swift s research group at L.A.N.L. is currently persuing a similar line of

3

Hot
exchanger ———
$\dot{Q}_H$

Prime mover
stack ———

Room temp.
exchangers ———
$\dot{Q}_R = \dot{Q}_H + \dot{Q}_C$

Heat pump
stack ———

Cold
exchanger ———
$\dot{Q}_C$

37 cm

Figure 2: The heat driven acoustic cooler. High-temperature heat causes low
temperature refrigeration (Swift, 1988)

investigation for a thermoacoustic generator. A five inch diameter, four meter long prime mover has been built and operated in a rigid-rigid resonator. The system is operated at a mean pressure of twenty atmospheres with helium as the working fluid. Acoustic pressures on the order of ten percent of the mean pressure have been observed. Acoustic power generated is on the order of one kilowatt.

The next phase of the development of an acoustic generator, using the five inch engine, is to obtain a transducer able to convert the acoustic energy to electrical energy. Two contractors, Mechanical Technology Inc. of Latham, New York and Sun Power Inc. of Athens, Ohio have been requested to provide quotations for delivery of a linear alternator for this purpose. The cost of such a device has been estimated at between $25,000 (Sunpower) and $115,000 (MTI). Because of the high cost (and current lack of funding) it was decided that a computer program should be developed in the interim, which would predict the performance of the combined prime mover-transducer system. In addition, such a program, once experimentally validated, could be used to determine the effect of changing the geometry or material of the stack assembly, the position of the stack assembly in the resonator, or the characteristics of the mechanical or electrical load on the performance of the system as a whole. Such a program could result in a great deal of savings in material and man hours when design modifications are contemplated.

II. THEORY

A. THERMODYNAMICS

In designing any heat engine, compromises are made between thermodynamic ideals, and engineering and marketing realities. In designing any device, a practical balance is sought between the desire for high efficiency, power, and reliability and the necessity of achieving low cost, small size and maximum simplicity. Thermoacoustic engines are extremely simple devices, as will be seen, and promise to deliver a substantial fraction of the ideal thermoacoustic efficiency.

In any basic thermodynamics course we learn that there are two principle types of heat engines: heat pumps and prime movers. A heat pump removes heat Q_C from a low temperature reservoir at temperature T_C, receives work W from the surroundings, and delivers heat Q_H to a high temperature sink at temperature T_H.

The process is reversed in a prime mover. Heat Q_H is received from a high temperature reservoir at temperature T_H, work W is done on the surroundings, and the remaining heat Q_C is dumped to a low temperature sink at temperature T_C.

The first and second laws of thermodynamics place an upper limit on the efficiency of any heat engine. This limit is best understood by applying the Carnot cycle to the process. The Carnot cycle was first introduced in 1824 by N. L. Sadi Carnot (Sears and Salinger, 1975). The Carnot cycle (Fig. 4) consists of two reversible isothermal processes and two reversible adiabatic processes. The direction of the cycle (i.e. clockwise or counter-clockwise) determines whether the engine is a prime mover or a heat pump. Since the work in this thesis deals solely with prime movers, the remainder of the discussion in this section will focus on them.

From the first law of thermodynamics we know that energy must be conserved in the system. It follows that

$$Q_H - Q_C = W. \tag{1}$$

The second law requires that the total entropy in the system must increase or remain constant. The change in entropy for isothermal heat transport to/from a resorvoir is given by
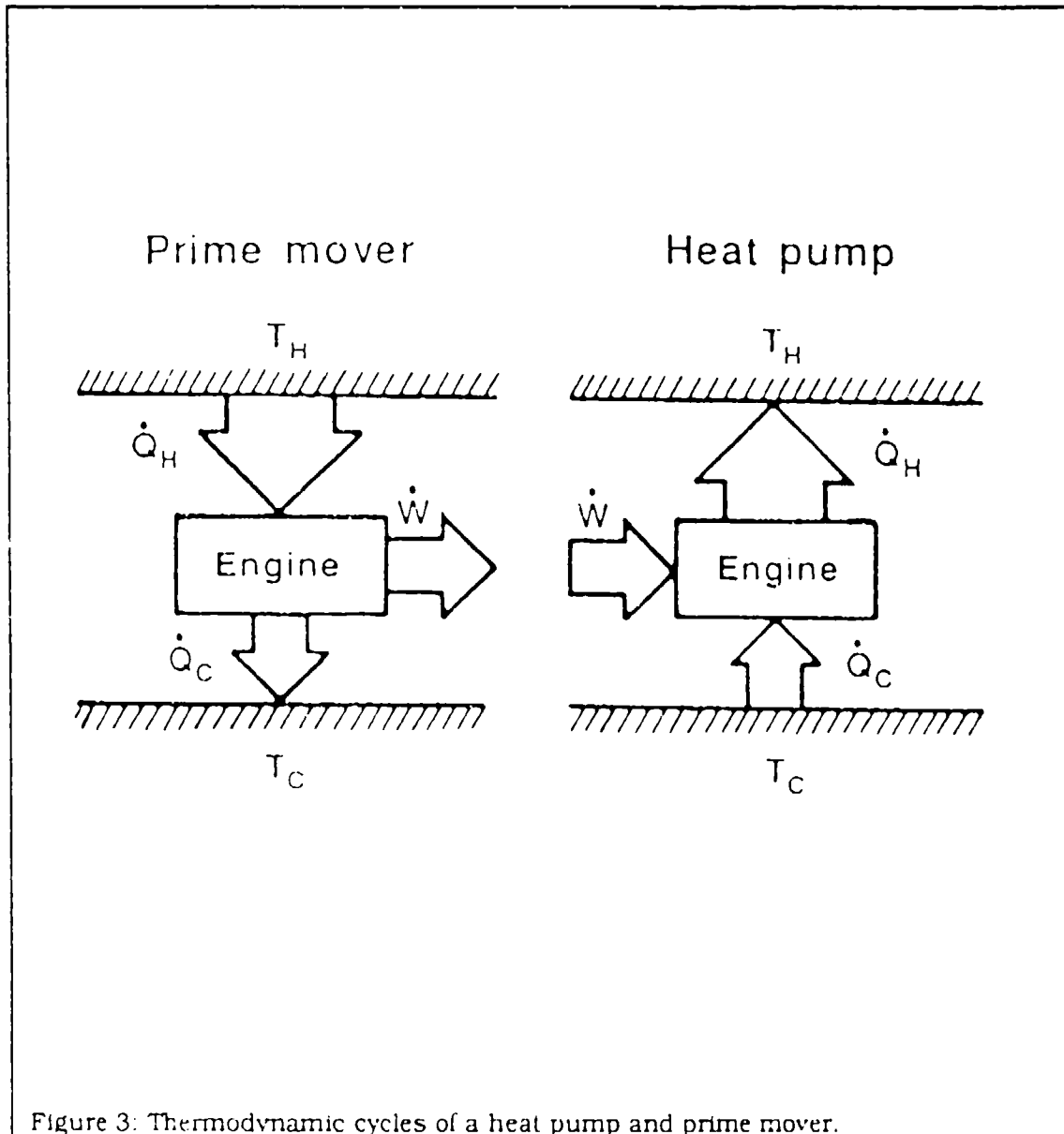

Figure 3: Thermodynamic cycles of a heat pump and prime mover.

$$\Delta S = Q/T. \tag{2}$$

For a prime mover the second law may be written as

$$\Delta S_C - \Delta S_H = Q_C/T_C - Q_H/T_H \geq 0. \tag{3}$$

The efficiency of interest in a prime mover (the work output divided by the heat input) is

$\eta = W/Q_H$. Combining Eqs. 1 and 3 it can be shown that

$$\eta = W/Q_H \leq (T_H - T_C)/T_H \tag{4}$$

The temperature ratio on the right side of the above equation is known as Carnot's

efficiency $(\eta_c = (T_H - T_C)/T_H)$ and is the highest efficiency that a prime mover can

achieve.

Figure   4:   The   Carnot   cycle   (Sears   and   Salinger,   1975)
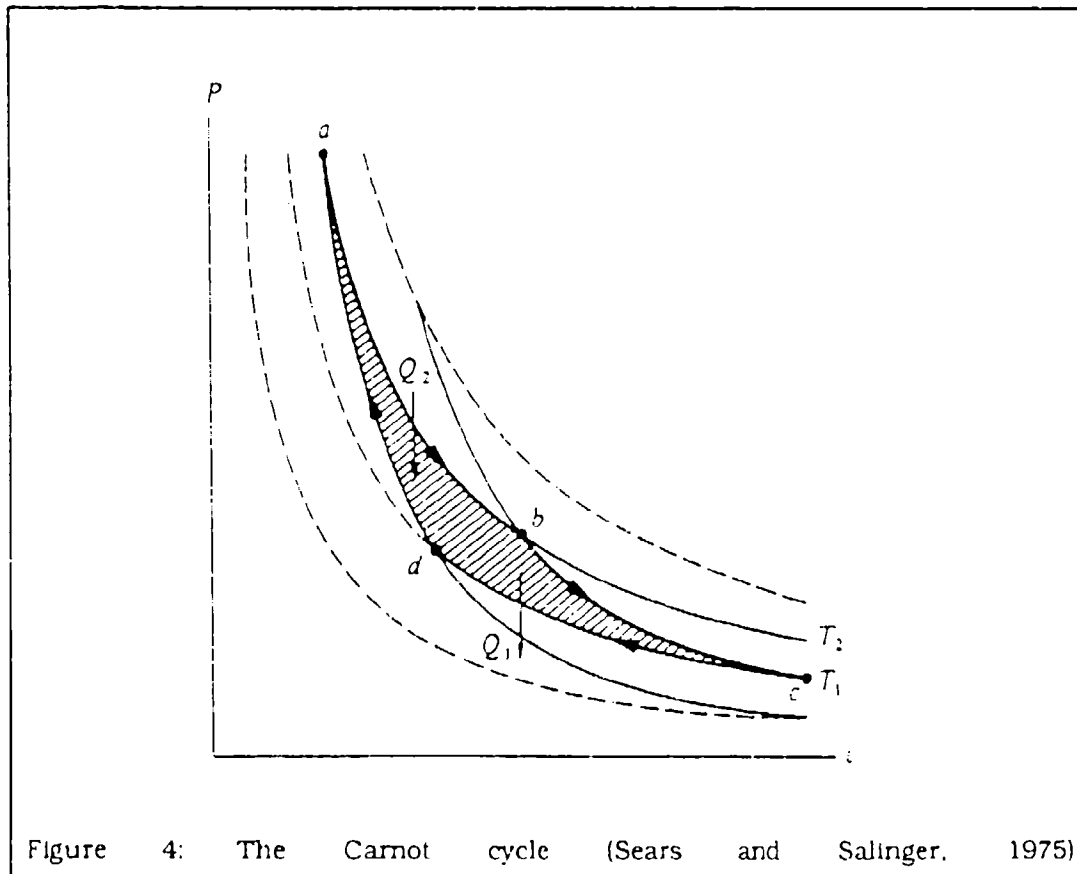
B. THERMOACOUSTIC THEORY

As stated in Chapter 1, thermoacoustic theory was developed in detail by Rott and others in the late 1960's and 1970's. Since then, a great deal of work has been done by Swift, Hofler, Wheatley, and others in applying Rott's theory to experimental devices. The work contained in this thesis relies heavily on the relationships developed by applying the short stack and boundary layer approximations to the most general of thermoacoustic derivations (Swift, 1988).

1. A Qualitative Picture

Consider a gas parcel in thermal contact with and oscillating along a plate at the acoustic frequency (Fig. 5). As the gas parcel moves back and forth, it will experience changes in pressure, volume, and temperature. The temperature change is due to both the adiabatic compression and expansion of the gas by the acoustic pressure and by the local temperature of the plate.

Consider first the gas parcel in motion along a plate with no temperature gradient (Fig. 5a). The gas parcel starts at position 1 with a temperature T. The acoustic wave moves the parcel to the right a distance dx to position 2 and compresses it adiabatically, raising its temperature to T^{++}. The temperature of the gas is now higher than the local temperature of the plate so heat Q flows from the gas to the plate, causing the plate to warm up at position 2 and the gas to cool to temperature T^+. As the gas cools its volume decreases, so that work is done on the parcel by the surrounding gas. The gas parcel now moves back to position 1, undergoing adiabatic expansion. It arrives at position 1 with a temperature T^-, which is lower than the local plate temperature. The result is a heat flow from the plate to the gas parcel. The increase in temperature of the gas parcel causes it to expand, resulting in work being done by the parcel on the surrounding gas. As this cycle is repeated, the constant dumping of heat at position 2 and the removal of heat from position 1 results in a temperature gradient across the plate and heat transfer to the right along the plate.
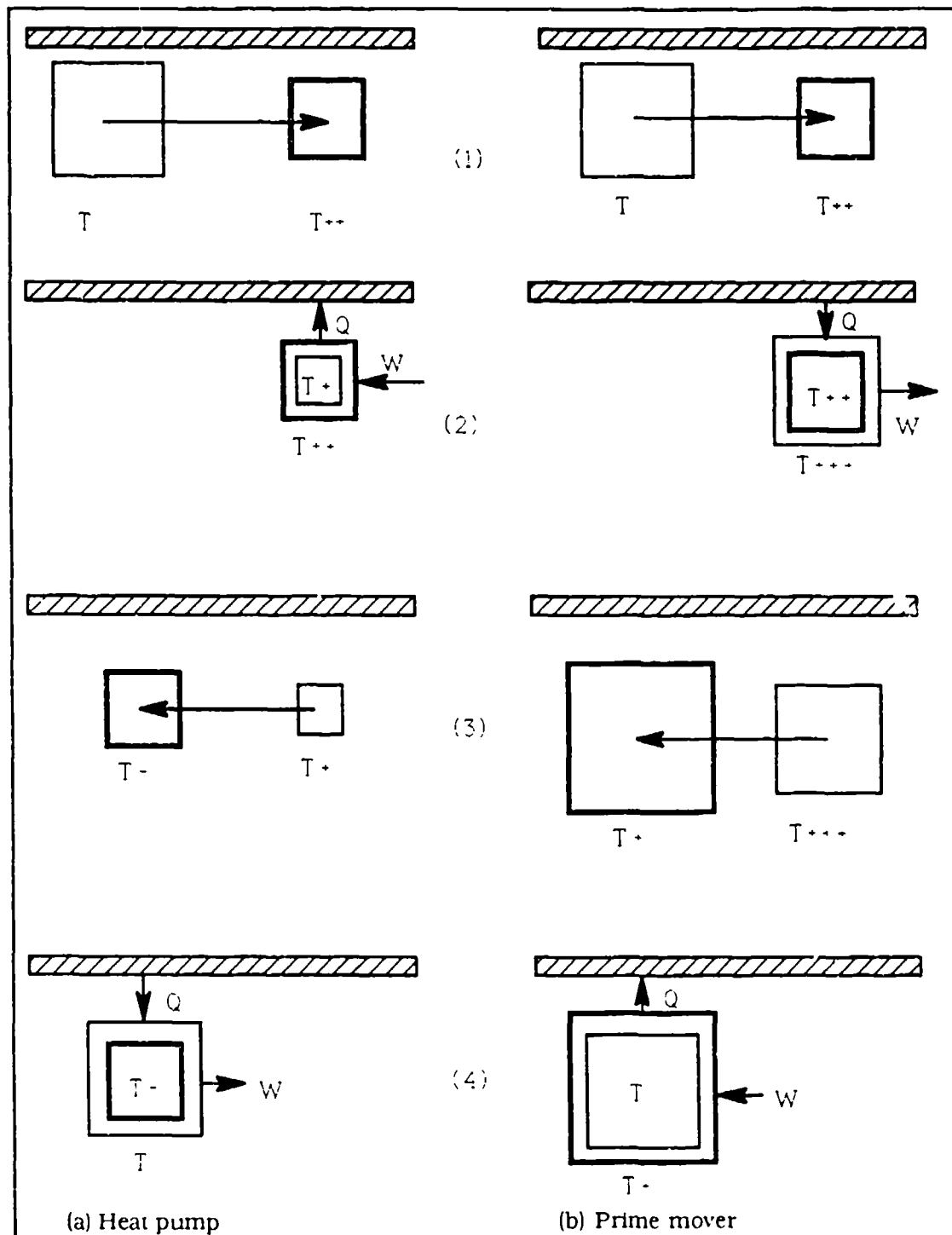
9

Figure 5: Fluid parcels in (a) a thermoacoustic heat pump and (b) a prime mover. Steps 1 and 3 are adiabats while 2 and 4 are isochors.

Next, consider the cycle for a prime mover (Fig. 5b). Assume a temperature gradient (∇T) is maintained along the plate by means of heat exchangers located at either end of the plate, with the hot heat exchanger located to the right. Now when the gas parcel is compressed adiabatically and moved from position 1 to position 2, heat will flow from the plate to the gas parcel as long as $T + dx(\nabla T) > T^{++}$. This process will result in an expansion of the gas parcel as it is heated to a temperature T^{+++}, so that work is done on the surrounding gas. When the gas is then adiabatically expanded and moved back to position 1 it will be at temperature T^+. Heat must then flow from the gas to the plate and work will be done on the parcel by the surrounding gas. Heat is thus pumped from the hot heat exchanger to the cold heat exchanger.

The actual process is sinusoidal rather than articulated as described above. As we shall see later, the heat transfer takes place only within a thermal penetration depth of the surface of the plate. This thermal penetration depth (δ_κ) is the distance heat can diffuse through the gas in a time equal to the reciprocal of the angular frequency at which the motion is taking place. Thermoacoustic engines may be thought of as a long train of adjacent gas parcels, all within about a thermal penetration depth of the surface of the plate, that draw heat from the plate at one extreme of their motion, and deposit heat at the other extreme (Wheatley, Swift, and Migliori, 1986).

2. The Single Plate

The basic principles of thermoacoustic engines are most clearly illustrated by examining the simple case of a single, small solid plate aligned parallel to the direction of vibration of a standing acoustic wave. The presence of the plate in the standing wave modifies the wave, resulting in (1) a time-averaged heat flux near the surface of the plate, along the direction of the acoustic vibration and (2) the generation or absorption of real acoustic power near the surface of the plate. These two simple effects are the basis of all thermoacoustic engine phenomena (Swift, 1988). The

following discussion follows Swift's paper closely. The only significant difference is that we have chosen to model the acoustic pressure as a cosine function so that the resulting expression for fluid particle velocity contains a sine term.

In the absence of the plate, the pressure and x-direction velocity of the standing wave have well known acoustic properties. Let the fluid pressure be given by

$$p = pm + p1e^{j\omega t} \tag{5}$$

where the acoustic pressure is given by

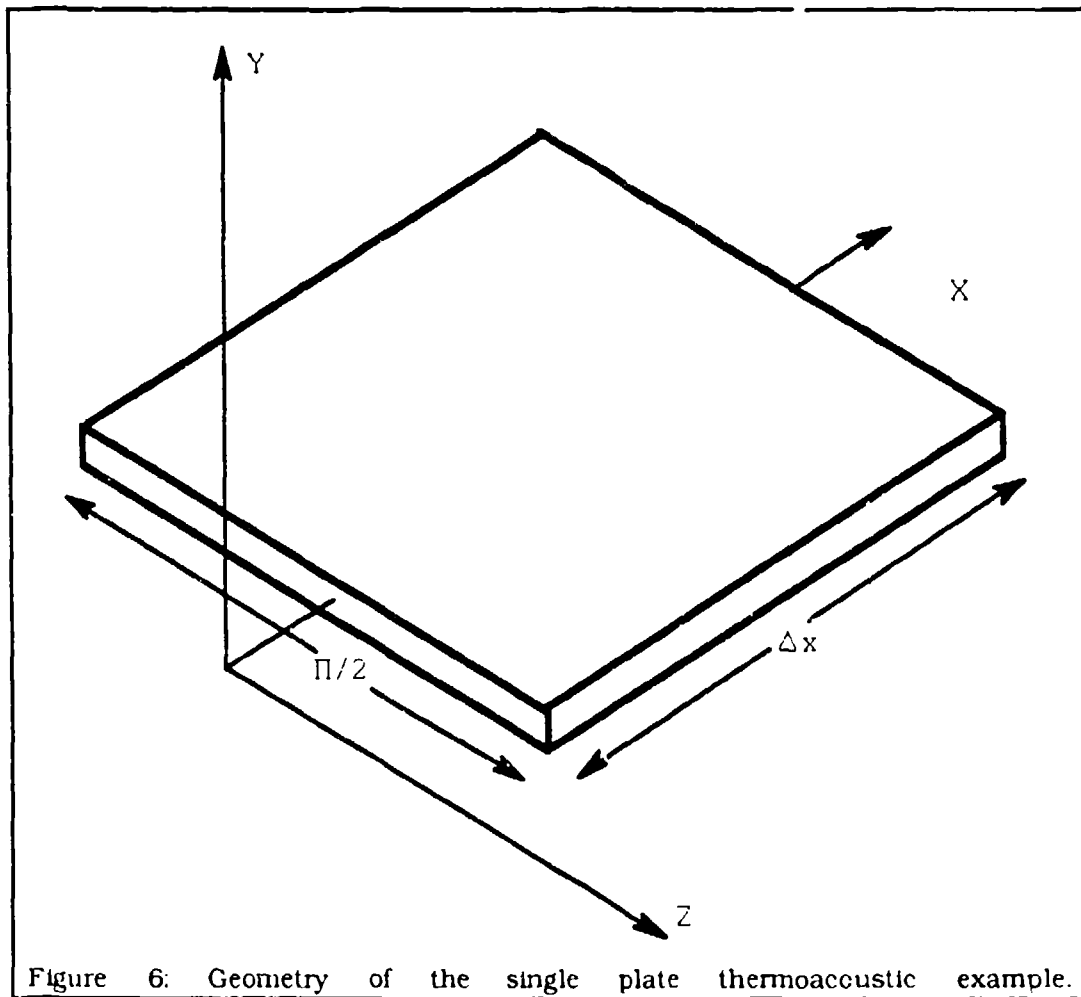$$p1 = P_0 \cos(kx) \equiv p_1{}^S(x). \tag{6}$$

Figure 6: Geometry of the single plate thermoacoustic example.

12

The fluid particle velocity is found by applying the linear inviscid force equation (Kinsler and others, 1982) to Eq. 5. The result is

$$u = u_1 e^{j\omega t}, \tag{7}$$

where

$$u_1 = -i(P_0/\rho_m c)\sin(kx) = -iu_1{}^S(x). \tag{8}$$

In the absence of the plate, the sound wave is adiabatic and has an oscillating temperature given by

$$T_1 = (T_m\beta/\rho_m c_p)p_1. \tag{9}$$

For an ideal gas we know

$$T_m\beta/\rho_m c_p = (\gamma-1)T_m/\gamma p_m. \tag{10}$$

Combining Eqs. 9 and 10 it can be shown that

$$T_1/T_m = [(\gamma-1)/\gamma]p_1/p_m \tag{11}$$

for ideal gases. Thus the fractional temperature oscillations are of the same order of magnitude as the fractional pressure oscillations.

The introduction of the plate into the standing wave modifies the unperturbed temperature oscillations due to the heat flow between the gas and the plate. The presence of the plate modifies the temperature oscillations in both magnitude and phase, for fluid within about a thermal penetration depth of the plate surface. The thermal penetration depth in the fluid is given by

$$\delta_\kappa = \sqrt{(2\kappa/\omega)}. \tag{12}$$

At this point it is prudent to make several assumptions that will facilitate the calculations which follow. These are:

(1) that steady state exists,
(2) the plate is short compared to the acoustic wavelength and that it is located far from both the pressure and velocity nodes so that both p_1 and u_1 can be considered uniform over the plate,

13

(3) the fluid is inviscid so that u_1 does not depend on y,

(4) the plate has a large enough heat capacity per unit area so that it's temperature does not change appreciably at the acoustic frequency,

(5) the thermophysical properties of the plate material and the gas are independent of temperature,

(6) the plate has a mean temperature gradient in the x direction ∇T_m and the plates thermal conductivity in the x direction is negligible,

(7) the fluids thermal conductivity in the x direction is also negligible,

(8) the mean fluid temperature is independent of y and is the same as that of the plate.

Calculation of the oscillating fluid temperature is accomplished using only the first order terms in the general equation of heat transfer, expressing the entropy in terms of the pressure and temperature of the fluid as

$$s_1 = (c_p/T_m)T_1 - (\beta/\rho_m)p_1,$$ (13)

and finally solving the resulting differential equation subject to the appropriate boundary conditions (Swift, 1988, p. 1151). The solution is

$$T_1 = [(T_m\beta/\rho_m c_p)p_1{}^s - (\nabla T_m/\omega)u_1{}^s][1 - e^{-(1+i)y/\delta_\kappa}].$$ (14)

To understand the terms of this equation, first take the limit as $\delta_\kappa << y$ where the fluid makes negligible thermal contact with the plate. Under this condition

$$T_1 \rightarrow (T_m\beta/\rho_m c_p)p_1{}^s - (\nabla T_m/\omega)u_1{}^s.$$ (15)

The first term is due to the adiabatic compression and expansion of the gas. The second term is a result of the mean temperature gradient in the fluid and the fact that the fluid oscillates in the x direction with displacement amplitude $u_1{}^s/\omega$. Setting $T_1 = 0$ and solving Eq. 15 for ∇T_m, we see that there is a critical mean temperature gradient

$$\nabla T_{crit} = T_m\beta\omega p_1{}^s/\rho_m c_p u_1{}^s$$ (16)

for which the temperature oscillations at a point are zero. This critical temperature gradient is important because it marks the boundary between the heat pump and the

14

prime mover regions of operation. Further manipulation of Eq. 16, using Eqs. 6 and 8, and the generalization of Eq. 10 to an arbitrary fluid leads to the useful result

$$\nabla T_{crit} = [(\gamma-1)/T_m\beta](T_m k) \cot(kx) \tag{17}$$

The exponential term in Eq. 14 is complex. It approaches zero for $y \ll \delta_\kappa$

where the plate imposes the boundary condition $T_1 = 0$. When $y \approx \delta_\kappa$ it has a substantial imaginary part. This phase shift in the oscillating temperature of the standing wave due to the presence of the plate leads directly to the time averaged heat flow in the x direction.

a   Heat Flux

Since we have assumed that thermal conductivity in both the plate and the gas is negligible in the x direction, the only way that heat can be transported in the x direction is by the hydrodynamic transport of entropy, thus the heat flux per area is given by

$$q_2 = T_m\rho_m<s_1 u_1>. \tag{18}$$

Substituting Eq. 13 for s_1 and simplifying results in an expression for heat flow as a function of y. The total heat flux Q_2 along the plate in the x direction can then be found by integrating q_2 over the y-z plane. The resulting expression is

$$Q_2 = -(1/4)\Pi\delta_\kappa T_m\beta p_1{}^s u_1{}^s(\Gamma-1) \tag{19}$$

where $\Gamma = \nabla T_m/\nabla T_{crit}$ is the ratio of actual temperature gradient to critical temperature gradient. The term $T_m\beta$ is nearly 1 for ideal gases and the term $\Pi\delta_\kappa$ is the area which is thermodynamically active in a plane perpendicular to the plate. The heat flux will be

zero if the plate is positioned at either a pressure or a velocity node of the standing wave which is readily understood from the product $p_1{}^S u_1{}^S$. Finally we see that if $\nabla T_m = \nabla T_{crit}$ then $\Gamma = 1$ and no heat flux occures. If $\nabla T_m < \nabla T_{crit}$, then $\Gamma - 1 < 0$ and the heat flux is toward the velocity node. If $\nabla T_m > \nabla T_{crit}$, then $\Gamma - 1 > 0$ and the heat flux is toward the pressure node. If suitable heat exchangers are positioned at the ends of the plate, the heat flux carries heat from one heat exchanger to the other.

b. Work Flux

The work flux, or acoustic power is derived in a similar manner from thermodynamic principles. The work done by a differential volume element of fluid in going from a volume dx dy dz to a volume dx dy dz + dV is

$$dw = p \, dV = - (p/\rho) \, dx \, dy \, dz \, d\rho, \tag{20}$$

so the power per unit volume is

$$w = - (p/\rho) \, d\rho/dt. \tag{21}$$

Since, for oscillatory motion, we are interested in the time average work flux we use Eq. 5 for p and

$$d\rho/dt = i\omega\rho_1 + u_1(\partial\rho_m/\partial x) \tag{22}$$

to find

$$w_2 = - (\omega/\rho_m) <i p_1 \rho_1> \tag{23}$$

for the average acoustic power produced (or absorbed) per unit volume. After expressing ρ_1 in terms of T_1 and p_1 and substituting into Eq. 22 we finally arrive at the result

$$w_2 = - (1/2) \, \omega\beta p_1{}^S \, Im\{T_1\}. \tag{24}$$

Just as with the heat flux per area, only the imaginary part of the temperature oscillations contributes to the acoustic power produced per unit volume. The fluid within about a thermal penetration depth of the surface of the plate "breaths" because of

16

thermal expansion or contraction, with the correct time phase with respect to the oscillating pressure to do or absorb net work.

By integrating w_2 over all space, using Eq. 14 for T_1, the total acoustic power produced is found to be

$$W2 = (1/4)\Pi\delta\kappa\Delta x(T_m\beta^2\omega/\rho_m c_p)(p_1{}^s)^2(\Gamma-1).\tag{25}$$

This acoustic power is proportional to the volume of the fluid, $\Pi\delta\kappa\Delta x$, that is within a thermal penetration depth of the plate. It is also quadratic in the acoustic amplitude and vanishes at the pressure nodes. Finally it is proportional to the same temperature gradient factor $\Gamma-1$ as appeared in the expression for the total heat flux. Whether this power increases the amplitude of the standing wave, is radiated away to infinity, or flows through an acoustic-to-electric transducer to generate electric power depends on the details of the resonator.

c. *Efficiency*

The efficiency of the single plate engine, used as a prime mover is given by $\eta = W/Q_H$. For a short plate, Q_2 is essentially constant with x, so $Q_H = Q_c = Q_2$. Substituting for W_2 and Q_2 from Eqs. 19 and 25 above results in the expression

$$\eta = \Delta x\beta\omega p_1{}^s/\rho_m c_p u_1{}^s.\tag{26}$$

Using the definition of ∇T_{crit}, this equation can be recast into the form

$$\eta = \eta_c/\Gamma.\tag{27}$$

Thus we see that as $\Gamma \rightarrow 1$, the single plate engine approaches Carnot's efficiency, but this is also the point where the power output of the engine approaches zero.

3. The Short Engine

In the previous section, thermoacoustic effects were examined for the simple case of a single plate in an acoustic standing wave. In order to examine these effects

without a great deal of distractions, several simplifying assumptions were made. The central thermoacoustic effects that were revealed are:

(1) The thermal boundary condition imposed on the fluid by the plate causes a phase shift of the oscillating temperature of the fluid within a thermal penetration depth of the plate.
(2) Heat flows hydrodynamically, parallel to the plate in the fluid about a thermal penetration depth from the plate.
(3) Acoustic power is absorbed or produced by the fluid about a thermal penetration depth from the plate.
(4) The direction of heat flow, and whether power is produced or absorbed, depends on the magnitude of the mean-temperature gradient relative to the critical temperature gradient.

We now turn our attention to the more realistic model of an engine built with a stack of parallel plates. The two sets of coordinate axis used in the detailed calculations (Swift, 1988, pp.1176-1179) which are summarized below are indicated in Fig. 7. We shall also discard many of our previous simplifying assumptions although we shall retain the assumptions that the temperature spanned is much less than the absolute temperature and that the length of the plates is much less than an acoustic wavelength.

Swift's derivation proceeds as follows. Consider a parallel plate engine geometry with the acoustic vibration along the x axis and the y axis perpendicular to the planes of the parallel plates. The equation of motion for the fluid is

$$\rho(\partial \mathbf{v}/\partial t + (\mathbf{v}\cdot\nabla)\mathbf{v})$$

$$= -\nabla p + \mu\nabla^2\mathbf{v} + (\xi+\mu/3)\nabla(\nabla\cdot\mathbf{v}). \tag{28}$$

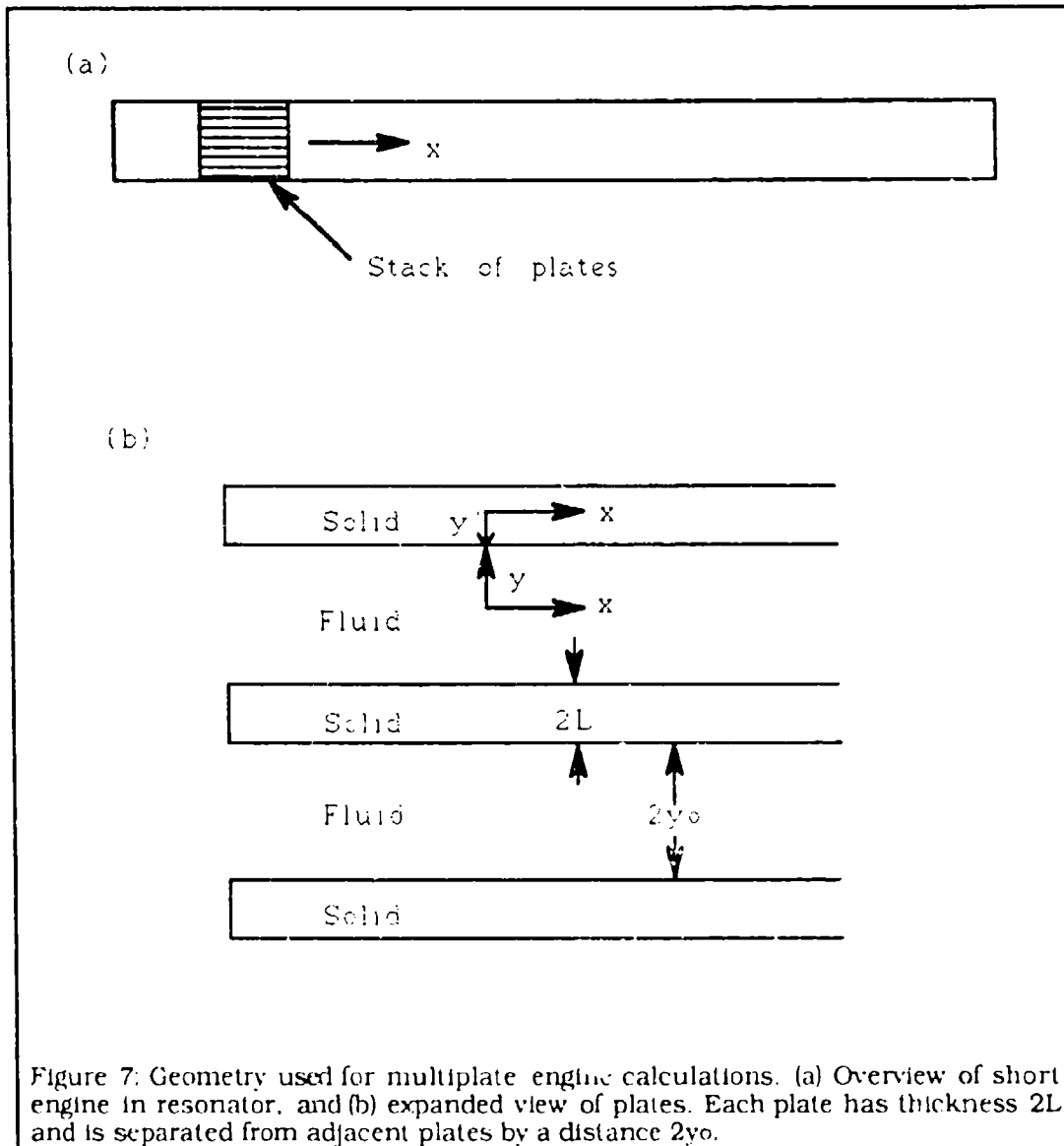with the boundary condition $\mathbf{v} = 0$ at the surface of the plates. The continuity equation for the fluid is

$$\partial\rho/\partial t + \nabla\cdot(\rho\mathbf{v}) = 0. \tag{29}$$

The equations for heat flow in the fluid and solid are

$$\rho T(\partial s/\partial t+\mathbf{v}\cdot\nabla s) = \nabla\cdot(K\nabla T)$$
$$+ \text{(terms quadratic in velocity)} \tag{30}$$

and $\qquad \rho_s c_s \partial T_s / \partial t = K_s \nabla^2 T_s,$ $\qquad\qquad\qquad$ (31)

with boundary conditions $T = T_s$ and $K \partial T / \partial y = K_s \partial T_s / \partial y$ at the fluid-solid interface. The above equations are linearized, assuming that each of the variables oscillates at angular frequency ω:

Figure 7: Geometry used for multiplate engine calculations. (a) Overview of short engine in resonator, and (b) expanded view of plates. Each plate has thickness 2L and is separated from adjacent plates by a distance 2yo.

$$p = p_m + p_1(x)e^{i\omega t}. \tag{32}$$

$$\rho = \rho_m(x) + \rho_1(x,y)e^{i\omega t} \tag{33}$$

$$\mathbf{v} = \mathbf{i}u_1(x,y)e^{i\omega t} + \mathbf{j}v_1(x,y)e^{i\omega t}. \tag{34}$$

$$T = T_m(x) + T_1(x,y)^{i\omega t}. \tag{35}$$

$$T_s = T_m(x) + T_{s1}(x,y)^{i\omega t}. \tag{36}$$

$$s = s_m(x) + s_1(x,y)^{i\omega t}. \tag{37}$$

Integrating the resulting equations with respect to y yields a wave equation for $p_1(x)$ in terms of dT_m/dx and material properties and geometry, and an equation for energy flux H_2 (which includes both heat and work) along x in terms of $p_1(x)$, $T_m(x)$, material properties, and geometry. The wave equation is

$$\{1+(\gamma-1)f_\kappa/(1+\varepsilon_s)\}p_1 + (\rho_m c^2/\omega^2)d/dx\{[(1-f_v)/\rho_m]dp_1/dx\}$$

$$- (\beta c^2/\omega^2)\{[(f_\kappa-f_v)/\{(1-\sigma)(1+\varepsilon_s)\}](dT_m/dx)(dp_1/dx) = 0, \tag{38}$$

where

$$f_v = \tanh[(1+i)y_0/\delta_v]/\{(1+i)y_0/\delta_v\}. \tag{39}$$

$$f_\kappa = \tanh[(1+i)y_0/\delta_\kappa]/\{(1+i)y_0/\delta_\kappa\}. \tag{40}$$

$$\varepsilon_s = \rho_m c_p \delta_\kappa \tanh[(1+i)y_0/\delta_\kappa]/\rho_s c_s \delta_s \tanh[(1+i)L/\delta_s]. \tag{41}$$

$$\delta_v = \sqrt{(2v/\omega)}. \tag{42}$$

$$\delta_\kappa = \sqrt{(2\kappa/\omega)}. \tag{43}$$

and $\qquad \delta_S = \sqrt{(2\kappa_S/\omega)}.$ (44)

The term δ_S is the thermal penetration depth in the solid, and is analogous to the thermal penetration depth in the fluid discussed previously, while δ_v is the viscous penetration depth of the fluid. The viscous penetration depth is roughly the distance shear diffuses in a time $1/\omega$. The equation for energy flux is

$$H_2 = (\Pi y_0/2\omega\rho_m)Im[(dp_1^*/dx)p_1(1-f_v^*-T_m\,\beta(f_\kappa-f_v^*)/\{(1+\sigma)(1+\varepsilon_s)\})]$$

$$+ (\Pi y_0 c_p/2\omega^3\rho_m(1-\sigma))(dT_m/dx)(dp_1/dx)(dp_1^*/dx)$$

$$X\ Im[f_v^*+[(f_\kappa-f_v^*)(1+\varepsilon_s(f_v/f_\kappa)/\{(1+\sigma)(1+\varepsilon_s)\})]$$

$$- \Pi(y_0K+LK_s)(dT_m/dx).$$ (45)

In order to make contact with the single plate results, we make three assumptions designed to simplify the equations. These assumptions are zero viscosity, the "boundary-layer" approximation, and the "short-stack" approximation. (The assumption that the fluid viscosity is zero is not a good approximation in most realistic situations, requiring that the viscous terms be ut back into the equations at a later time.) With the fluid viscosity set equal to zero the terms σ and f_v both vanish.

The "boundary-layer" approximation consists of the assumptions that $y_0>>\delta_\kappa$ and that $L>>\delta_s$. The goal of these assumptions is to set the hyperbolic tangents equal to unity. This is reasonable for cases where the value of the dimension of interest is at least twice the value of the associated boundary layer (i.e. $y_0 \geq 2\delta_\kappa$)(Swift, 1988).

The "short-stack" approximation assumes that the stack is short enough that it does not appreciably disturb the standing wave, so that we can take

$$p_1 = P_0\cos(kx) \equiv p_1^s$$ (46)

21

and

$$u_1 = -i(1+L/y_0)(P_0/\rho_m c)\sin(kx) \equiv -iu_1^s. \tag{47}$$

These are the same expressions used in the single plate calculations except for the term $1+L/y_0$ which is required for continuity of volume velocity. It is further assumed that the stack is short enough that p_1^s and u_1^s may be regarded as independent of x within the stack, and that $\Delta T = T_H - T_C \ll T_m$, so that thermophysical properties can be assumed independent of T_m and hence of x.

With these assumptions, and using the equation

$$dp_1/dx = -\omega\rho_m u_1^s, \tag{48}$$

(Swift, 1988, p. 1158) we obtain

$$H_2 = -(1/4)\Pi\delta_\kappa[T_m\beta p_1^s u_1^s/(1+\epsilon_s)][\Gamma-1]$$

$$- \Pi(y_0 K + L K_s)(dT_m/dx) \tag{49}$$

for energy flux, and

$$p_1 + (\rho_m c^2/\omega^2)d/dx\{(1/\rho_m)dp_1/dx\}$$

$$= [(\gamma-1)\delta_\kappa p_1/\{(1+l)(1+\epsilon_s)y_0\}](\Gamma - 1) \tag{50}$$

for the wave equation.

The acoustic power generated (or absorbed) in the stack may be determined by multiplying the change in average acoustic intensity between the two ends of the stack by the fluid cross section at the stack exit. The resulting equation is

$$W_2 = \Pi y_0[<p_1 u_1>_{\text{right}} - <p_1 u_1>_{\text{left}}]$$

$$= \Pi y_0\Delta x d(<p_1 u_1>)/dx. \tag{51}$$

Manipulating Eq. 51, using Eqs. 48 and 50, we find that

$$W_2 = (1/4)\Pi\delta_\kappa\Delta x[(\gamma-1)\omega/\{\rho_m c^2(1+\epsilon_s)\}](p_1{}^s)^2(\Gamma-1) \qquad (52)$$

We pause now to make contact with the simple results of the single plate calculations. We begin by examining the energy flux equation. The first term on the right in Eq. 49 differs from the right side of Eq. 19 by a factor $1/(1+\epsilon_s)$ which accounts for the finite heat capacity of the plates and modifies the boundary condition for temperature at the fluid-solid interface. The second term on the right side of Eq. 49 accounts for ordinary heat conduction in the plates and the fluid. Upon examination of the equations for work flux (Eqs. 25 and 52) we find that the difference is again the factor $1/(1+\epsilon_s)$ described above.

We now include viscosity and repeat the above calculations, but now use the relationship

$$dp_1/dx = -\omega\rho_m u_1{}^s/(1-f_v) \qquad (53)$$

(Swift, 1988, p. 1159). Notice that dp_1/dx is now complex due to the presence of viscosity in the fluid. (Note that Eqs. 46 and 47 may still be used for this case as long as we now let $u_1{}^s$ represent the mean fluid velocity in the x direction. Due to the presence of viscosity, the x component of the fluid velocity is a function of y, going from zero at the surface of the plates to some maximum value at a distance on the order of a viscous penetration depth away from the plates.) We now obtain

$$H_2 = -1/4\Pi\ \delta_\kappa[T_m\beta p_1{}^s u_1{}^s/\{(1+\sigma)(1+\epsilon_s)(1-\delta_v/y_o+\delta_v{}^2/2y_o{}^2)\}]$$

$$X\ [\Gamma\{1+\sqrt{\sigma}+\sigma+\sigma\epsilon_s)/(1+\sqrt{\sigma}) - (1+\sqrt{\sigma}-\delta_v/y_o)]$$

$$-\ \Pi(y_oK+LK_s)(dT_m/dx) \qquad (54)$$

for energy flux, and

$$p_1 + (\rho_m c^2/\omega^2)d/dx\{[(1-f_v)/\rho_m]dp_1/dx\}$$

$$= (\gamma-1)\delta_\kappa p_1/\{(1+i)(1+\varepsilon_s)y_0\}[\Gamma/\{(1+\sqrt{\sigma})(1-f_v)\} - 1] \qquad (55)$$

for the wave equation.

The work flux is calculated in the same manner as before and the result is

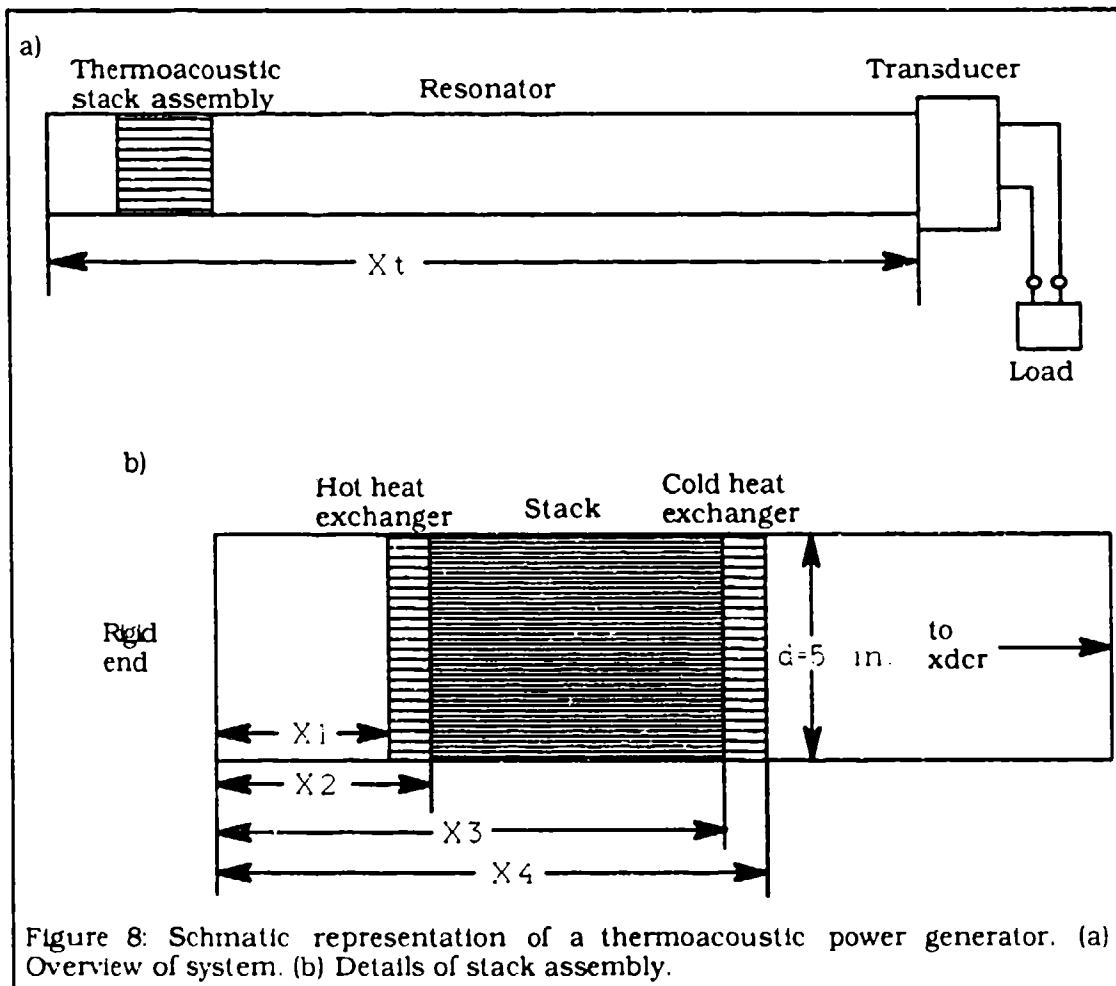$$W_2 \quad = (1/4)\Pi\delta_\kappa\Delta x\{[(\gamma-1)\omega(p_1{}^s)^2/(\rho_m c^2(1+\varepsilon_s))\}$$

$$X \{\Gamma/\{(1+\sqrt{\sigma})(1-\delta_v/y_0+\delta_v{}^2/2y_0{}^2)\} - 1\}$$

$$- (1/\dot{}_i)\Pi\delta_v\Delta x\{\omega\rho_m(u_1{}^s)^2/(1-\delta_v/y_0+\delta_v{}^2/2y_0{}^2). \qquad (56)$$

It is clear that the inclusion of viscosity in the calculations adds significant complexity to the results, and the intuitive understanding of the components of the equations is lost.

III. DESCRIPTION O ? APPARATUS

The apparatus which we are modeling in this thesis is a thermoacoustic prime mover, enclosed in a rigid tube resonator, driving an acoustic-to-electric power transducer. Figure 8 is a general schematic of the device. Specific values of the dimensions of the prime mover are contained in Table 1.
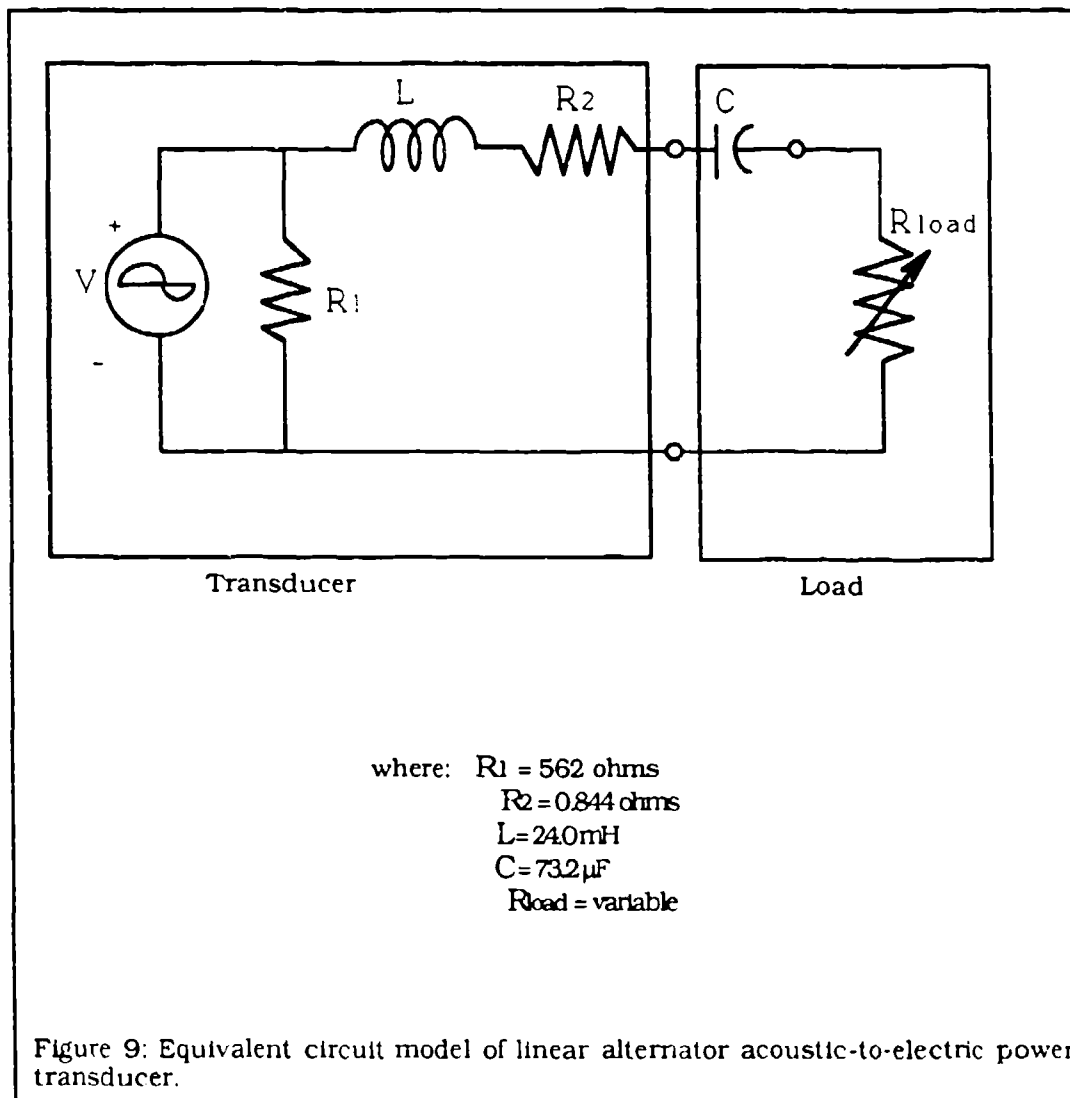
The transducer proposed for use in this application is a linear alternator. Design requirements submitted for bid by Dr. Greg Swift of L.A.N.L. include 1 kW of power

Figure 8: Schmatic representation of a thermoacoustic power generator. (a) Overview of system. (b) Details of stack assembly.

Characteristic / Device	Hot heat exchanger	Thermo-acoustic stack	Cold heat exchanger
Inlet position relative to rigid end (m)	0.305	0.356	0.584
Exit position relative to rigid end (m)	0.356	0.584	0.635
Plate thickness (m)	4.57e-4	1.27e-4	2.54e-4
Fluid gap (m)	9.40e-4	7.94e-4	7.94e-4
Material	N i	304 SS	Cu
K (W/m K)	89.9	16.3	350.0
Cp (J/Kg K)	443.8	451.9	384.0
Density (Kg/m^3)	8890	8027	8900

Table 1: Summary of geometry of thermoacoustic stack assembly and important thermodynamic parameters.

delivered to an electric load resistance of 3 to 100 ohms with at least 60% efficiency when driven by a 4 bar peak-to-peak pressure amplitude at 120 Hz in helium at a mean pressure of 20 bar. The details of the proposals received in response to the request for quotation contain proprietary information. The transducer model used in this thesis was designed with the assistance of Nick Vitale of MTI. Although it does not represent the actual design proposal submitted by MTI, it should provide reasonable approximations for the performance of the prime mover-transducer system. The transducer may be modeled by the equivalent circuit indicated in Fig. 9. The moving mass of the transducer is 0.766 Kg, the spring constant is 1.43E5 Kg/s^2, the magnetic field strength is 0.97 Tesla, and the coil has a total effective length of 32.6 m. The mechanical resistance of the transducer is 2.0 Kg/s. Although the actual transducer will have some physical limitation to its displacement, we have not imposed any such limitation on our model.

where: R1 = 562 ohms
        R2 = 0.844 ohms
        L = 24.0mH
        C = 73.2 μF
        Rload = variable

Figure 9: Equivalent circuit model of linear alternator acoustic-to-electric power transducer.

IV. NUMERICAL MODEL

In order to formulate a program capable of modeling the performance of our thermoacoustic generator, we must identify the parameters which may be allowed to vary during the operation of the device, and then develop a system of equations that will relate these variables. The geometry of the device will be fixed. It is assumed that the thermodynamic properties of the material used in the construction of the device will not vary significantly over the range of pressures and temperatures at which the device will operate. It is further assumed that the temperature of the cold heat exchanger will be constant. The working fluid used will be a mixture of helium and argon gases. The mixture of these gases will be determined so as to achieve a 120 Hz operating frequency at a median load resistance of 13 ohms. The parameters that will be allowed to vary in the model are the acoustic pressure amplitude, angular frequency, and the temperature of the hot heat exchanger, for a given input heat flux and load resistance. Variation of the hot end temperature will result in variation of the thermodynamic properties of the working fluid and of the sound speed in the fluid.

Before continuing, one additional assumption will be made concerning the performance of the system; specifically, that no attenuation occurs in the resonator. All acoustic power generated in the stack must therefore be removed at the transducer. This assumption is made to simplify the calculations, but is not truely valid since a significant fraction of the acoustic power would be attenuated due to thermal and viscous effects at the walls of the resonator.

We now begin to develop the equations which will determine the performance of the system using the short stack and boundary layer approximations discussed previously. Starting at the rigid end of the resonator, and assuming a standing wave, we know that the pressure amplitude must be at a maximum and the fluid particle velocity

must be zero. We can therefore describe the pressure and fluid particle velocity in the region between the rigid end and the stack assembly using Eqs. 6 and 8, which are repeated below for ease of reference.

$$p(x) = P_0 \cos(kx) \tag{6}$$

$$u(x) = -i(P_0/\rho_m c) \sin(kx) \tag{8}$$

The short stack approximation allows us to assume that the pressure amplitude in the stack is constant. Using the mean stack position to determine the value of this term we find

$$p(x_m) = p_1{}^s = P_0 \cos(k_m x_m) \tag{57}$$

where $\quad k_m = \omega/c_m.$ $\tag{58}$

and c_m is the mean sound speed in the system. The mean fluid particle velocity at the mean stack position is given by

$$u(x_m) = -iu_1{}^s = -ig(P_0/\rho_m c) \sin(k_m x_m), \tag{59}$$

where $g = 1+L/y_0$ is the geometry factor necessary to maintain continuity of volume velocity. It must be noted that g has different values for the stack and the two heat exchangers.

The change in acoustic pressure due to the stack and heat exchangers is obtained from Eq. 53. The resulting equations are

$$dp_{ht} = -P_0 \omega dx_{ht} g_{ht} \sin(k_m x_m)/(c_m(1-f_{v,ht})). \tag{60}$$

$$dp_{st} = -P_0 \omega dx_{st} g_{st} \sin(k_m x_m)/(c_m(1-f_{v,st})). \tag{61}$$

and $\quad dp_{cd} = -P_0 \omega dx_{cd} g_{cd} \sin(k_m x_m)/(c_m(1-f_{v,cd})). \tag{62}$

where $\quad f_v = 1/((1+i)y_0/\delta_v). \tag{63}$

Note the subscripts indicating the parameters which have different values depending

on the location in the stack assembly. The acoustic pressure at the exit of the stack assembly is then the sum of the pressure changes in the stack and the pressure at the stack entrance:

$$p(x_4) = p(x_1) + dp_{ht} + dp_{st} + dp_{cd} \tag{64}$$

where
$$p(x_1) = P_0 \cos(k_{ht}x_1). \tag{65}$$

The change in mean fluid particle velocity is obtained from the wave equation (Eq. 55) by substituting for dp_1/dx from Eq. 53 and solving for du. The resulting equation is

$$du_1 = i[\omega p_1 dx/(\rho_m c^2)]$$

$$X \{[(\gamma-1)\delta_\kappa/((1+i)(1+\epsilon_s)y_0)][\Gamma/((1+\sqrt{\sigma})(1-f_v))-1]-1\}. \tag{66}$$

The changes in mean fluid particle velocity in the heat exchangers and the stack are then

$$du_{ht} = i[\omega P_0 dx_{ht} \cos(k_m x_m)/(\rho_m c_m^2)]$$

$$X \{[(\gamma-1)\delta_\kappa/((1+i)(1+\epsilon_{s,ht})y_{0,ht})][\Gamma/((1+\sqrt{\sigma})(1-f_{v,ht}))-1]-1\}, \tag{67}$$

$$du_{st} = i[\omega P_0 dx_{st} \cos(k_m x_m)/(\rho_m c_m^2)]$$

$$X \{[(\gamma-1)\delta_\kappa/((1+i)(1+\epsilon_{s,st})y_{0,st})][\Gamma/((1+\sqrt{\sigma})(1-f_{v,st}))-1]-1\}. \tag{68}$$

and

$$du_{cd} = i[\omega P_0 dx_{cd} \cos(k_m x_m)/(\rho_m c_m^2)]$$

$$X \{[(\gamma-1)\delta_\kappa/((1+i)(1+\epsilon_{s,cd})y_{0,cd})][\Gamma/((1+\sqrt{\sigma})(1-f_{v,cd}))-1]-1\}. \tag{69}$$

The fluid particle velocity at the stack exit is

$$u(x_4) = u(x_1) + du_{ht}/g_{ht} + du_{st}/g_{st} + du_{cd}/g_{cd} \tag{70}$$

where
$$u(x_1) = -i(P_0/r_m c_{ht}) \sin(k_{ht}x_1). \tag{71}$$

The geometry factors are required for continuity of volume velocity as before.

Assume now that the acoustic wave in the region between the stack assembly and the transducer has the form of left and right traveling plane waves described by

$$p(x,t) = Ae^{i(\omega t - kx)} + Be^{i(\omega t + kx)} \tag{72}$$

where A and B are complex coefficients given by

$$A = a + i\alpha \tag{73}$$

and $\qquad B = b + i\beta. \tag{74}$

The associated fluid particle velocity is found from Euler's equation to be

$$u(x,t) = (A/\rho_m c_{cd})e^{i(\omega t - kx)} - (B/\rho_m c_{cd})e^{i(\omega t + kx)}. \tag{75}$$

Dropping the time dependence of Eqs. 72 and 75, and expanding in terms of sines and cosines yields equations for acoustic pressure and fluid particle velocity in the resonator between the stack assembly and the transducer of the form

$$p(x) = (a+b)\cos(k_{cd}x) + (\alpha-\beta)\sin(k_{cd}x)$$

$$+ i[(\alpha+\beta)\cos(k_{cd}x) - (a-b)\sin(k_{cd}x)] \tag{76}$$

and

$$u(x) = (1/\rho_m c_{cd})\{(a-b)\cos(k_{cd}x) + (\alpha+\beta)\sin(k_{cd}x)$$

$$+ i[(\alpha-\beta)\cos(k_{cd}x) - (a+b)\sin(k_{cd}x)]\} \tag{77}$$

One set of boundary conditions for Eqs. 76 and 77 are given by our expressions for pressure and velocity at the stack assembly exit. This requires expansion of the expressions into real and imaginary parts so that we may form the equalities

$$(a+b)\cos(k_{cd}x) + (\alpha-\beta)\sin(k_{cd}x) = Re(p(x_l) + dp_{ht} + dp_{st} + dp_{cd}), \tag{78}$$

$$(\alpha+\beta)\cos(k_{cd}x) - (a-b)\sin(k_{cd}x) = Im(p(x_l) + dp_{ht} + dp_{st} + dp_{cd}). \tag{79}$$

$$(1/\rho_m c_{cd})\{(a-b)\cos(k_{cd}x) + (\alpha+\beta)\sin(k_{cd}x)\}$$

$$= \text{Re}\{u(x_t)+du_{ht}/g_{ht}+du_{st}/g_{st}+du_{cd}/g_{cd}\}. \qquad (80)$$

and $\qquad (1/\rho_m c_{cd})\{(\alpha-\beta)\cos(k_{cd}x)-(a+b)\sin(k_{cd}x)\}$

$$= \text{Im}\{u(x_t)+du_{ht}/g_{ht}+du_{st}/g_{st}+du_{cd}/g_{cd}\}. \qquad (81)$$

The boundary condition at the transducer required for resonance is that the reactance of the combined system must vanish:

$$\text{Im}\{Z_r + Z_m\} = 0. \qquad (82)$$

The mechanical impedance of the acoustic wave at the transducer position is given by

$$Z_r = (\pi d^2/4)\{p(x_t)/u(x_t)\}. \qquad (83)$$

The mechanical impedance of the transducer is found by applying Newton's second law to the transducer. The force acting on the transducer by the acoustic pressure is

$$F_t \quad = (\pi d^2/4)p(x_t) \qquad (84a)$$

Applying Newton's second law to the transducer gives

$$F_t \quad = m_t a + s\zeta + R_m u + BL_c I. \qquad (84b)$$

This equation may be recast by recognizing that

$$a = i\omega u, \qquad (85)$$

$$\zeta = -iu/\omega, \qquad (86)$$

and $\qquad I = BL_c u/Z_e. \qquad (87)$

where $\qquad Z_e = [1/R_1+1/\{R_2+R_{load}+i(\omega L-1/\omega C)\}]^{-1}. \qquad (88)$

The result is that the mechanical impedance of the transducer may be written as

$$Z_m = F_t/u = R_m +(BL_c)^2/Z_e +i(\omega m_t-s/\omega). \qquad (89)$$

We may find two more equations, necessary to fully constrain the 7 variables of interest, by recognizing that the conditions in the system are directly effected by the amount of heat flux in the stack, and that the power propagating from the stack

32

assembly must be removed at the transducer during steady state operation. Our sixth equation is therefore Eq. 54. The seventh equation is

$$\Pi_{ac} - \Pi_m - \Pi_e = 0 \tag{90}$$

where $\qquad \Pi_{ac} = (\pi d^2/8)\mathrm{Re}\{pu^*\},$ (91)

$$\Pi_m = (1/2)R_m\{uu^*\}, \tag{92}$$

and $\qquad \Pi_e = (1/2)\mathrm{Re}\{I^*V\}.$ (93)

The voltage produced by the transducer is

$$V = BL_c u. \tag{94}$$

Before describing the method used to find solutions to these equations, it is useful to summarize them and the variables of interest. The seven equations are

(1) $(a+b)\cos(k_c dx)+(\alpha-\beta)\sin(k_c dx) = \mathrm{Re}\{p(x_1)+dp_{ht}+dp_{st}+dp_{cd}\}.$

(2) $(\alpha+\beta)\cos(k_c dx)-(a-b)\sin(k_c dx) = \mathrm{Im}\{p(x_1)+dp_{ht}+dp_{st}+dp_{cd}\}.$

(3) $(1/\rho_m c_{cd})\{(a-b)\cos(k_c dx)+(\alpha+\beta)\sin(k_c dx)\}$

$\qquad = \mathrm{Re}\{u(x_1)+du_{ht}/g_{ht}+du_{st}/g_{st}+du_{cd}/g_{cd}\}.$

(4) $(1/\rho_m c_{cd})\{(\alpha-\beta)\cos(k_c dx)-(a+b)\sin(k_c dx)\}$

$\qquad = \mathrm{Im}\{u(x_1)+du_{ht}/g_{ht}+du_{st}/g_{st}+du_{cd}/g_{cd}\}.$

(5) $\mathrm{Im}\{Z_r + Z_m\} = 0$,

(6) $H_2 = -1/4\Pi\delta_\kappa[T_m\beta p_1{}^s u_1{}^s/\{(1+\sigma)(1+\varepsilon_s)(1-\delta_v/y_0+\delta_v{}^2/2y_0{}^2)\}]$

$\qquad X \; [\Gamma[(1+\sqrt{\sigma}+\sigma+\sigma\varepsilon_s)/\{(1+\sqrt{\sigma})\} - (1+\sqrt{\sigma}-\delta_v/y_0)]$

$\qquad - \Pi(y_0 K + LK_s)(d\Gamma_m/dx).$

and

(7) $\Pi_{ac} - \Pi_m - \Pi_e = 0$.

The variables for which we are to solve these equations simultaneously are the five pressure coefficients P_0, a, α, b, and β, the angular frequency ω, and the temperature of the hot heat exchanger T_{ht}. In order to accomplish this task effectively, it is necessary to expand the above equations in terms of the parameters of interest and to solve analytically for the real and imaginary parts of the equations indicated. This was accomplished using an algebraic manipulation software system called Derive: a Mathematical Assistant for Personal Computers. The details and results of the calculations are to long to present here.

Before we begin to solve these equations we must know the values of all the parameters that are not variables. The parameters that describe the geometry of the system and the characteristics of the load will be fixed at the beginning of the process. The parameters that describe the working fluid are dependent on the gas mix used and on the temperature at the hot heat exchanger. This temperature effects the values of the viscosity, thermal conductivity, and Prandtl number of the gas mix as well as the sound speed in the system, which in turn effects the gas mix that will be chosen in order to have resonance at the desired frequency. It is necessary therefore, to begin the calculations by guessing a value of the hot end temperature and, based on this guess, calculate the required gas parameters. We must then solve the equations to find a new hot end temperature, and then adjust the values of the gas parameters in an iterative cycle, until a self-consistent solution is obtained.

We begin the process by "guessing" a value for T_{ht}. Using this value we calculate the mean temperature gradient ∇T_m, the mean temperature in the stack T_m, the average system temperature T_{avg}, and the critical temperature gradient ∇T_{crit} using the

34

relations

$$\nabla T_m = (T_{ht} - T_{cd}) / dx_{st}. \tag{95}$$

$$T_m = (T_{ht} + T_{cd}) / 2. \tag{96}$$

$$T_{avg} = (x_2 T_{ht} + dx_{st} T_m + (x_5 - x_3) T_{cd}) / x_5. \tag{97}$$

and

$$\nabla T_{crit} = [(\gamma - 1) / T_m \beta](T_m k_m) \cot(k_m x_m). \tag{17}$$

where

$$k = \omega / c_m = \pi / x_t. \tag{98}$$

For this first approximation it is assumed that $T_m \beta \approx 1$ and $\gamma = 1.67$. Using the result of the above calculations we then determine the normalized temperature gradient

$\Gamma = \nabla T_m / \nabla T_{crit}$.

With the temperature parameters calculated above we now determine the first estimate of the gas mix required to obtain resonance at the desired frequency f_o. This is accomplished by using the expression for sound speed in a perfect gas

$$c = \sqrt{(\gamma r T)} \tag{99}$$

and estimating the required sound speed as $c = f_o \lambda = 2 f_o x_t$. The gas constant is given by

$$r = R / (F_{he} W_{he} + F_{ar} W_{ar}) \tag{100}$$

where R is the universal gas constant, F is the mole fraction of the gas indicated by subscript that is present, and W is the molar weight of the gas indicated by subscript. Since only the two gases are present in the system, we may write

$$F_{ar} = 1 - F_{he}. \tag{101}$$

Substituting Eqs. 100 and 101 into Eq. 99, and using $c = 2 f_o x_t$, we solve for the mole fraction of helium required:

$$F_{he} = 1 / (W_{he} - W_{ar}) [\gamma R T_{avg} / (2 f_o x_t)^2 - W_{ar}]. \tag{102}$$

From these results we calculate the molar weight of the binary gas mixture for future use:

$$W_{mix} = F_{he}W_{he} + F_{ar}W_{ar}. \tag{103}$$

Having established an approximation for the required gas mix, we next determine the isobaric and isochoric specific heat capacities of the gases at T_{avg}. This is done by two subroutines called 'HELIUM' and 'ARGON'. These subroutines are modifications of programs, written by Robert D. Mccarty at the National Bureau of Standards, to calculate the thermodynamic properties of these and other gases, using a form of the virial equation of state. The modifications to the programs consisted primarily of eliminating functions not required for this application, such as output to files and calculation of additional thermodynamic properties (internal energy, entropy, enthalpy, etc..), and modifying the input requirements so that the subroutines read temperature and pressure (the input parameters required) from the main program instead of from the screen in an interactive mode. In addition, the upper temperature limit in 'ARGON' was raised from 400 K to 1000 K. Comparison of data calculated in this extended temperature region was found to be in agreement with tabulated data contained in available tables of thermodynamic properties for argon. Using the output from the subroutines, the isobaric and isochoric specific heat capacities of the binary gas mix are determined:

$$c_{p,mix} = (c_{p,he}F_{he}W_{he} + c_{p,ar}F_{ar}W_{ar})/W_{mix} \tag{104}$$

and $$c_{v,mix} = (c_{v,he}F_{he}W_{he} + c_{v,ar}F_{ar}W_{ar})/W_{mix}. \tag{105}$$

From these, we then calculate a new value of the ratio of heat capacities, $\gamma = c_{p,mix}/c_{v,mix}$. If γ varies significantly from the initial value of 1.67, the gas mix is calculated again, using this new value, until a self consistent value is achieved.

Now that a reasonable gas mix has been established, and a value of the ratio of heat capacities determined, we can calculate the mean gas density and acoustic sound

speed in the resonator, assuming ideal gas behavior. The mean gas density is found using the ideal gas relation

$$\rho_m = p_m W_{mix}/RT_{avg}. \tag{106}$$

The acoustic sound speed in the resonator is found using Eq. 99.

Of more interest are the gas properties in the stack assembly, where the thermoacoustic effects are occurring. To determine these, we again use the subroutines 'HELIUM' and 'ARGON', but with T_m as the input temperature. We obtain the specific heat capacities of the two gases, calculate the specific heat capacities of the binary mixture, and determine γ and the acoustic sound speed for the stack assembly as described above for the resonator. To determine the dynamic viscosity, thermal conductivity, and Prandtl number of the binary gas mixture, we call subroutine 'PRANTL'. PRANTL is a modified version of a program written by a student at the Naval Postgraduate School (Susalla, 1988) to calculate these same parameters for thermoacoustic refrigerator design calculations. The original program calculated the dynamic viscosity, thermal conductivity, and Prandtl number for helium-argon and helium-xenon gas mixes at only two temperatures. The program was modified to allow for calculations over a range of temperatures, but only for helium-argon mixtures. The input parameters required for the subroutine are the temperature of interest and the isobaric specific heat capacities of the two gases.

Having now obtained the necessary parameters based on our first estimate of the hot end temperature, we are nearly ready to solve our seven equations. The seven equations which we must solve simultaneously are non-linear in the variables of interest, and can not easily be solved analytically. We chose instead, to use a readily available Fortran Library subroutine to find the solution for us. The subroutine used is the IMSL Library subroutine NEQNF. NEQNF is a single precision subroutine which uses The Levenberg-Marquardt algorithm and a finite-difference approximation to the Jacobian to solve a system of nonlinear equations.

In order to find the solution, the subroutine requires initial "guesses" for the values of the variables. We have established a "guess" for the hot heat exchanger temperature in order to estimate the gas properties above. The "guess" for the angular frequency is obviously $\omega = 2\pi f_0$. What is lacking are initial values of the pressure coefficients.

In previous work with the 5 inch engine at L.A.N.L., operating it in a simple rigid-rigid resonator, acoustic pressures on the order of 10% of the mean pressure have been observed. We will take this value for P_0. Values for a, α, b, and β may be obtained by analytically solving equations similar to Eqs. 78-81 derived from the inviscid relationships for the short engine. The resulting equations are too long to be repeated here. Initial "guess" values for a, α, b, and β are calculated in subroutine 'FIRST'.

Having determined all of the required input parameters, we now call the library subroutine to solve our system of equations for the seven "unknown" variables. If the resulting new hot end temperature differs significantly from the initial "guess" it is necessary to redo the calculations of the temperature dependent parameters and gas parameters (excluding the gas mix) and solve again. This process is repeated until the values of the hot heat exchanger temperature do not change significantly from one iteration to the next.

Once a consistent value of T_{ht} is determined, we compare the resulting angular frequency to our desired operating frequency. If the calculated frequency is higher than the design point, we increase the argon fraction, thereby reducing the acoustic sound speed, and repeat the iteration process. Conversly, if the frequency is too low, the argon fraction is reduced, and the iteration process repeated. These corrections are repeated until a gas mix is found which puts use near the desired operating frequency.

Finally we compare the electric power generated by the transducer (not that delivered to the load) with a desired maximum value. If the power generated differs

from the design value, H2 is adjusted and the entire iteration process is repeated.

The ultimate result of the above process is a gas mix that will result in operation of the system at the desired frequency, and provide the desired power output, for a given load resistance and a particular heat flux input.

It should be noted here that the above iterative processes are actually carried out in two stages. The first stage, accomplished in subroutine 'INITIAL', provides a rough estimate of the required values. Subroutine 'REFINE' takes these rough estimates and refines them to the final values.

Once the gas mix is determined, it is fixed and the system of equations may be solved repeatedly for a variety of input heat fluxes and load resistances to determine the response of the system about the design point. The instantaneous power delivered to the load by the transducer is given by

$$\Pi_i = VI. \tag{107}$$

The current flowing through the load resistor is given by

$$I = (V/Z) \sin(\omega t + \phi) \tag{108}$$

(Ohanian, 1985) where V is the voltage produced by the transducer given by Eq. 137, ϕ is the phase difference between the voltage and the current given by

$$\phi = \tan^{-1}[(1/\omega C - \omega L)/(R_2 + R_{load})]. \tag{109}$$

and Z is the impedance of the branch containing the load resistor given by the relation

$$Z = R_2 + R_{load} - i(\omega L - 1/\omega C). \tag{110}$$

After appropriate substitution and reduction we find that the time average power delivered to the load is

$$\Pi_{load} = 1/2(BL_c)^2 R_{load}(u^* u/Z^* Z) \cos(\phi). \tag{111}$$

The term $\cos(\phi)$ is very nearly unity for the values of L, C, and ω of interest, and is neglected in the calculations of Π_{load} in the program. We may now calculate the total

system efficiency as

$$\eta = \Pi_{load}/H_2.$$ (112)

V. RESULTS

In this chapter we will present the results of calculations made for various load resistances, input heat fluxes, and transducer positions. The trends of some important thermoacoustic variables are presented graphically. Since no experimental device comparable to the one modeled has been built, no comparison of theoretical and experimental data is possible. The complexity of the governing relationships makes intuitive prediction of the trends difficult.

A. VARIATION IN LOAD RESISTANCE AND INPUT HEAT FLUX

In order to investigate the effect of varying the load resistance and input heat flux, we first fix the transducer position at 4.0 m. We then calculate the gas mix required for resonance at 120 Hz, with a nominal load resistance of 13.0 Ω. The result of these calculations is a gas mix of 97% helium and 3% argon.

Table 2 contains some representative values of important parameters calculated

Load Resistance (Ω)	Angular Frequency (rad/s)	Hot End Temp. (K)	Useful Power Generated (W)	Overall Efficiency (%)	Acoustic Pressure Amplitude (Bar)
8	769	1150	600	12	1.25
9	766	1100	589	11.8	1.26
10	764	1060	577	11.5	1.29
11	762	1030	565	11.3	1.31
12	760	1000	552	11	1.33
13	758	974	528	10.8	1.34
14	757	951	527	10.5	1.37
15	755	931	514	10.3	1.4
16	754	913	502	10	1.41
17	753	897	491	9.8	1.44

Table 2: Values of critical parameters as a function of load resistance for a 97% helium gas mix. The transducer is at 4.0 m and the input heat flux is constant at 5 kW.

41

for an input heat flux of 5 kW. Figures 10 through 14 indicate graphically the general trends of these parameters as the load is increased. Figure 15 shows the variation in acoustic pressure amplitude as a function of input heat flux for a number of load resistances. The output of the program indicated no variation in frequency, hot end temperature, or efficiency as the input heat flux was changed ᶠ ⸱ a given load resistance so no plots of these relationships are presented.

B. VARIATION IN TRANSDUCER POSITION

Calculations were also done for transducer positions of 3.5, 3.0, and 2.5 meters. Table 3 and the figures which follow indicate the general trends in the parameters of interest as the transducer is moved closer to the thermoacoustic stack.

We clearly expect the argon percentage to increase so that we maintain a resonant system. It is unclear what effect this will have on the overall performance of the system. Changing the ratio of argon to helium will certainly change the thermodynamic properties of the gas mix, but whether that change will be adverse or beneficial is not intuitively obvious.

Examining the following figures, we see that the normalized temperature gradient increases, the pressure amplitude increases, and the system efficiency decreases as the resonator is shortened for the same stack geometry.

The increase in the normalized temperature gradient as the transducer is moved closer to the stack assembly may be understood by noting that the concurrent change in

Xdcr Posit (m)	Helium Fraction (mole %)	Thermal Penetration Depth (mm)	Viscous Penetration Depth (mm)	Acoustic Pressure Amplitude (Bar)	Norm. Temp. Grad.	System Eff. (%)
4	97	0.219	0.165	1.83	3.443	10.8
3.5	92	0.212	0.152	1.87	3.572	10.4
3	84	0.202	0.138	1.93	3.787	9.66
2.5	70	0.186	0.124	2.03	4.207	8.52

Table 3: Effect of decreasing resonator length on parameters of interest.

the gas mix results in a decrease in the sound speed and thermal penetration depth of the gas. These decreases result in an increase in the temperature gradient in order to produce the same amount of acoustic power.
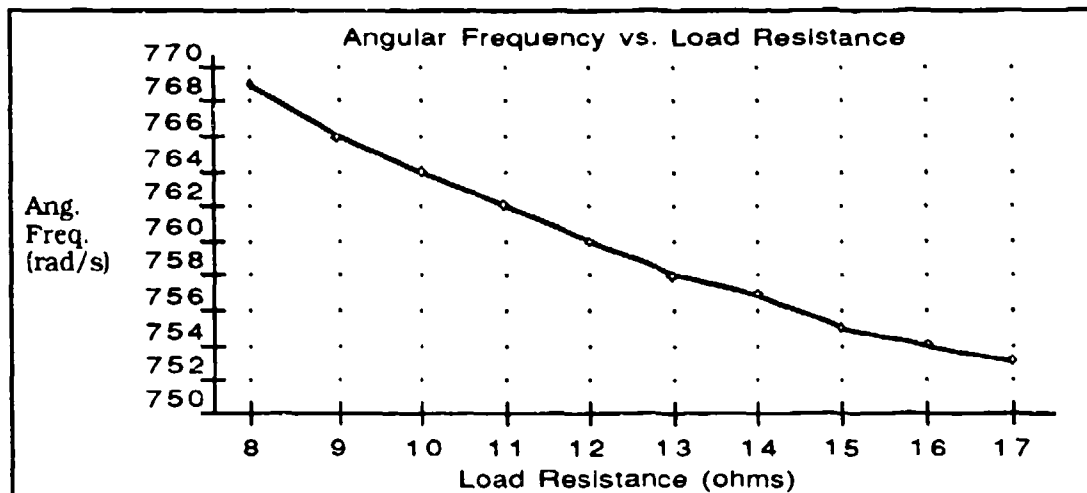
Figure 10: Plot of the variation of angular frequency with increasing load resistance for a 97% helium gas mix. The transducer is at 4.0 m and the input heat flux is 5 kW.
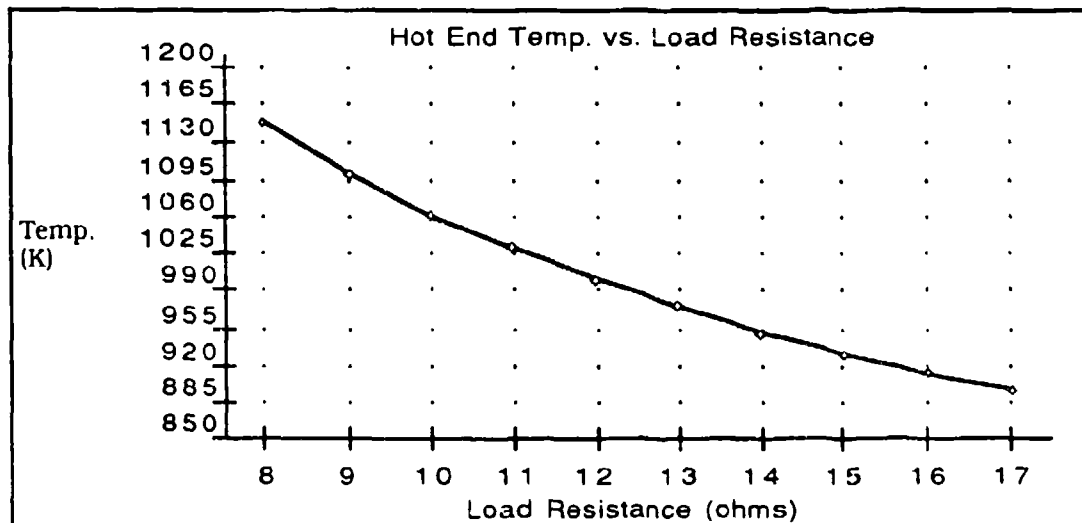

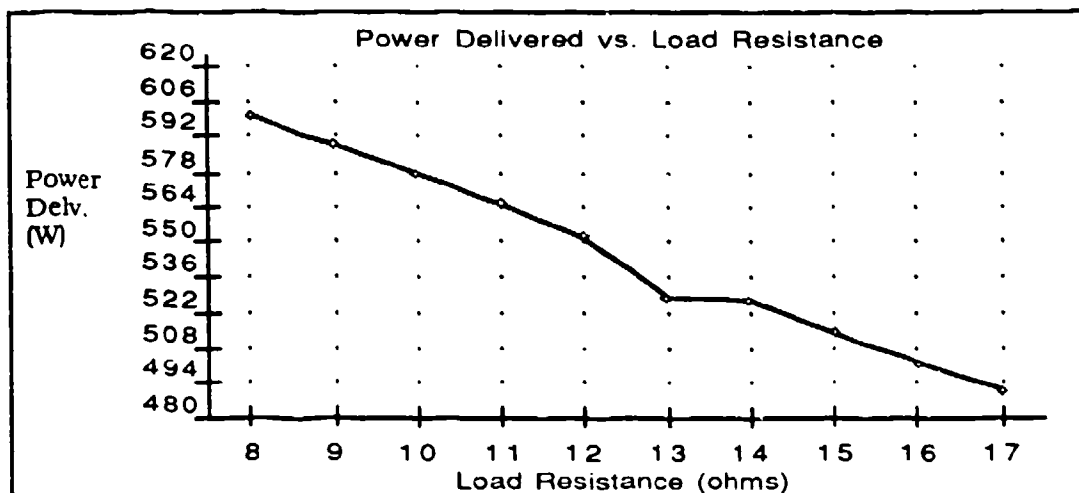Figure 11: Variation of hot heat exchanger temperature with load resistance for Xt = 4.0 m., H2 = 5 kW.

Figure 12: Plot of power dissipated in the load resistor as a function of the load resistance at a constant input heat flux of 5kW.
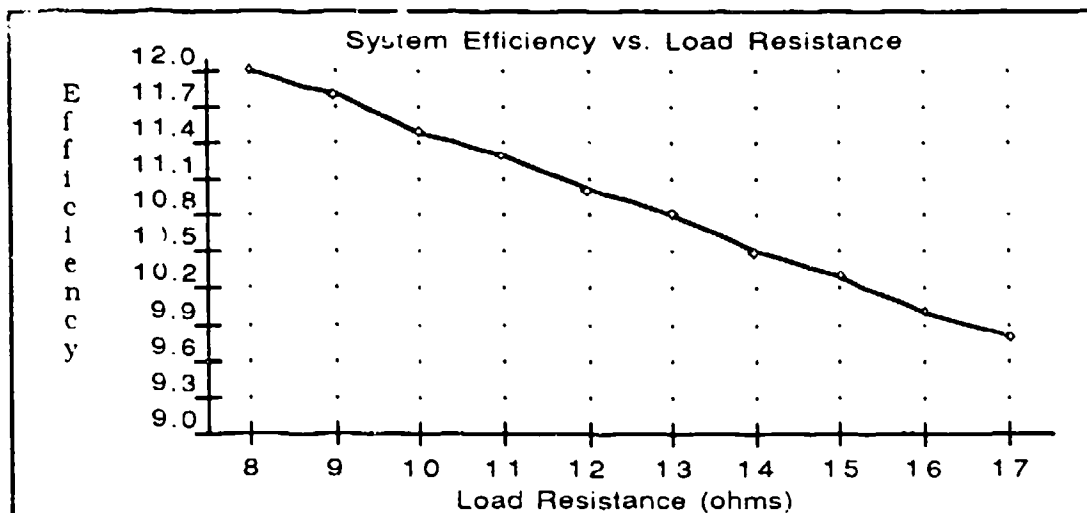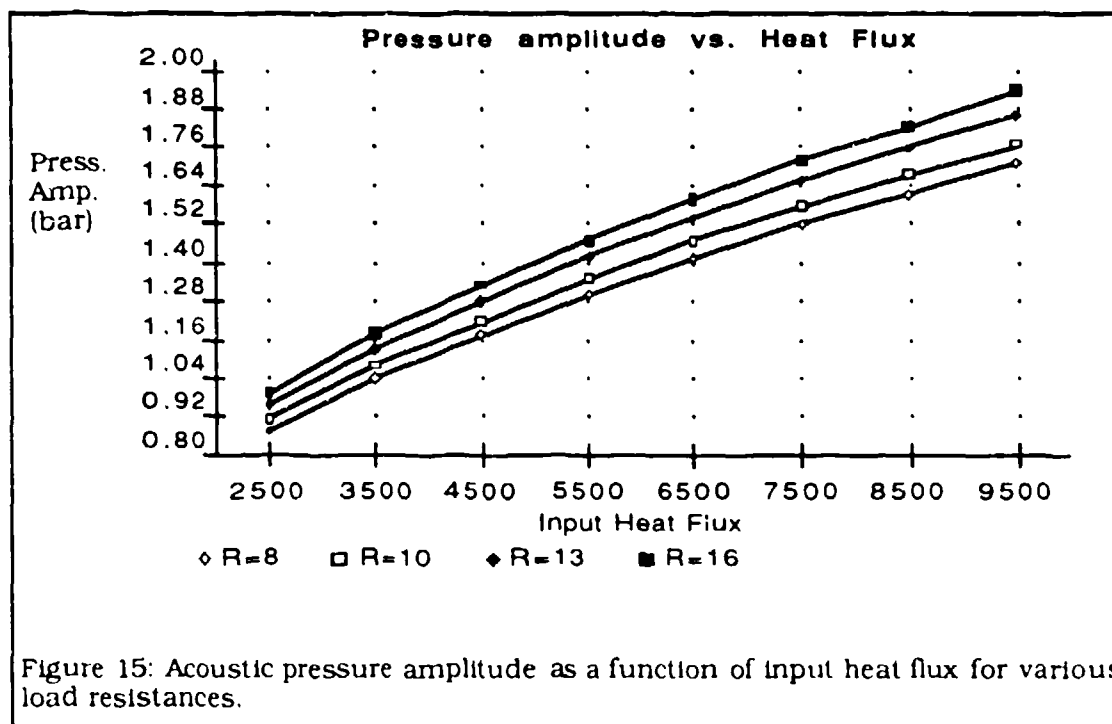

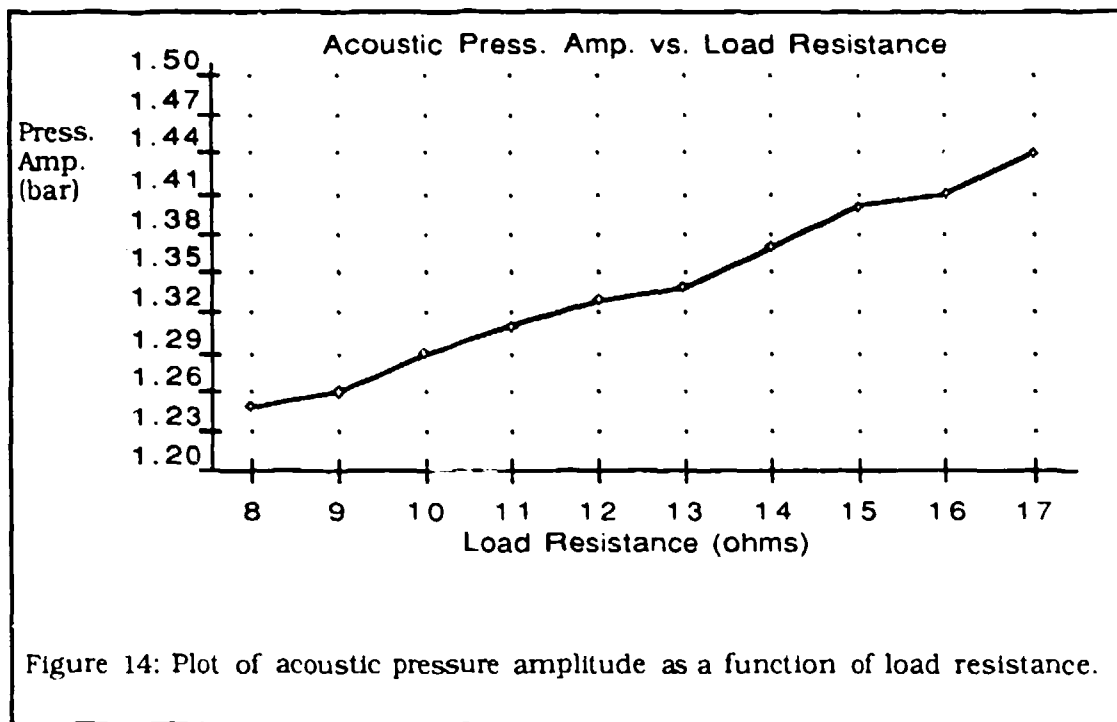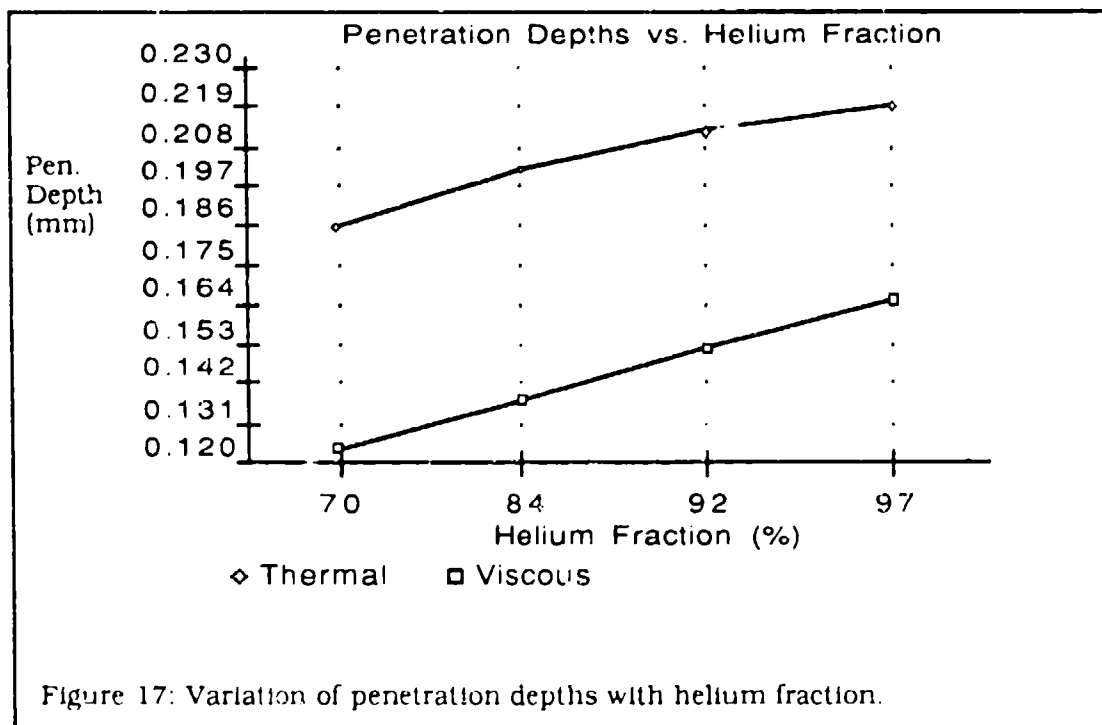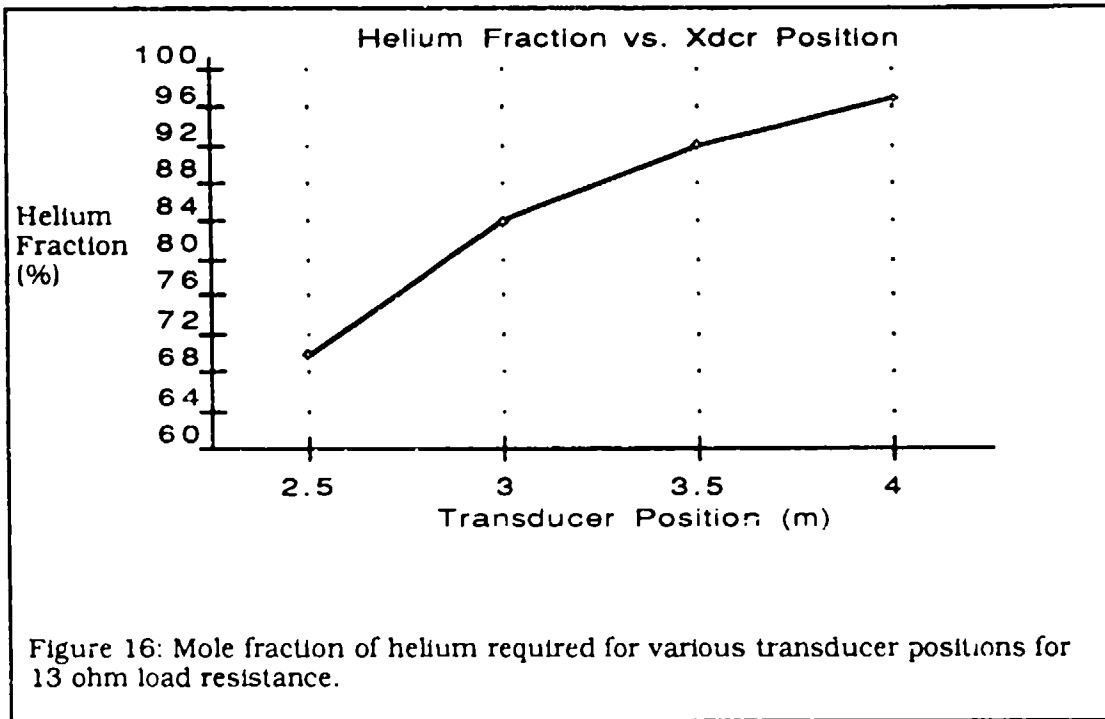Figure 13: Variation in system efficiency as a function of load resistance at constant heat flux.

Figure 14: Plot of acoustic pressure amplitude as a function of load resistance.

Figure 15: Acoustic pressure amplitude as a function of input heat flux for various load resistances.

Figure 16: Mole fraction of helium required for various transducer positions for 13 ohm load resistance.

Figure 17: Variation of penetration depths with helium fraction.

47

Figure 18: Variation in acoustic pressure amplitude as a function of transducer position to produce 1.1 kW of total electric power.

Figure 19: Normalized temperature gradient as a function of transducer position required to produce 1.1 kW of total electric power.

Figure 20: System efficiency as a function of transducer position.

VI. CONCLUSIONS AND RECOMMENDATIONS

It is not always obvious that the trends indicated by the figures in the proceeding chapter are those which we should expect. The lack of a working thermoacoustic generator for comparison does not allow for experimental validation of the results obtained. The results are of the correct order of magnitude, but the details of the relationships require additional investigation. It seems that a reasonable framework has been established for a model.

One way in which the program may be improved is by inclusion of viscous and thermal effects in the resonator. If this were done then the transducer parameters could be adjusted so that its mechanical impedance would be equivalent to that of a rigid end. Comparison of the output of the program to existing experimental data would then be possible. This may serve to validate the output of the program to some degree.

The next requirement is that a thermoacoustic generator be built and tested. It need not be as large as the five inch engine at L.A.N.L. to measure general performance trends. If the program is modified as suggested abovr hen a much smaller device in which the viscous and thermal effects in the resonat are substantial may be as easily modeled. A smaller device, working at a much lower pressure would not require such an expensive transducer.

REFERENCES

Hofler, T., *Thermoacoustic Refrigerator Design and Performance*, Ph.D. Dissertation, Physics Department, University of California at San Diego, 1986.

Susalla, M. P., *Thermodynamic Improvements for the Space Thermoacoustic Refrigerator (STAR)*, Masters Thesis, Naval Postgraduate School, Monterey, California, June 1988.

Putnam, A. A., and Dennis, W. R., *Survey of Organ-pipe Oscillations in Combustion Systems*, J. Acoust. Soc. Am., v. 28, p. 246, 1956.

Swift, G. W., *Thermoacoustic Engines*, J. Acoust. Soc. Am., v.84(4), pp. 1145-1180, October 1988.

Sears, F. W., and Salinger, G. L., *Thermodynamics, Kinetic Theory, and Statistical Thermodynamics*, 3d ed., Addison-Wesley Publishing Company, 1975.

Kinsler, L. E., and others, *Fundamentals of Acoustics*, 3d ed., John Wiley and Sons, Inc. 1982.

Hirschfelder, J. O., Curtiss, C. F., and Bird, R. B., *Molecular Theory of Gases and Liquids*, 2d printing, John Wiley and Sons, Inc., 1964.

Ohanian, H. C., *Physics*, W. W. Norton and Company, 1985.

BIBLIOGRAPHY

Hilsenrath, J., and others, *Tables of Thermodynamic and Transport Properties of Air, Argon, Carbon Dioxide, Carbon Monoxide, Hydrogen, Nitrogen, Oxygen, and Steam,* Pergamon Press, 1960.

Reif, F., *Fundamentals of Statistical and Thermal Physics,* McGraw-Hill Book Company, 1965.

Reitz, J. R., Milford, F. J., and Christy, R. W., *Foundations of Electromagnetic Theory,* 3d ed., Addison-Wesley Publishing Company, 1979.

Wheatly, J. C., *Intrinsically Irreversible or Natural Engines,* Tipografia Compositori Bologna, 1986.

Wheatly, J. C., Swift, G. W., and Migliori, A., *The Natural Heat Engine,* Los Alamos Science, Fall 1986.

Wilson, O. B., *Introduction to Theory and Design of Sonar Transducers,* Peninsula Publishing, 1985.

INITIAL DISTRIBUTION LIST

		No. of copies
1.	Defense Technical Information Center Cameron Station Alexandria, Virginia 22304-6145	2
2.	Library, Code 0142 Naval Postgraduate School Monterey, California 93943-5002	2
3.	Chairman, Department of Physics (Code 61) Naval Postgraduate School Monterey, California 93943-5002	1
4.	Professor A. A. Atchley Code 61Ay Naval Postgraduate School Monterey, California 93943-5002	5
5.	Dr. T. J. Hofler, Code 61Hf Naval Postgraduate School Monterey, California 93943-5002	1
6.	Dr. G. W. Swift Condensed Matter and Thermal Physics (P-10) Los Alamos National Lab Los Alamos, New Mexico 87545	2
7.	Professor S. Garrett, Code 61Gx Naval Postgraduate School Monterey, California 93943-5002	1
8.	Professor S. Baker, Code 61Bk Naval Postgraduate School Monterey, California 93943-5002	1
9.	Dr. Henry E. Bass Physical Acoustics Research Laboratory University of Mississippi University, Mississippi 38677	1
10.	Peter Ceperley Department of Physics George Mason University 4400 University Drive Fairfax, Virginia 22030	1

11.	James R. Belcher	1
	Department of Physics
	University of Mississippi
	University, Mississippi 38677

12.	Lt. Paul D. Fisher	2
	Department Head Class 115
	Surface Warfare Officers School Command
	Newport, Rhode Island 02841-5012